1	Circadian regulation of the transcriptome in a complex polyploid crop
2	
3	Hannah Rees <sup>1</sup> , Rachel Rusholme-Pilcher <sup>1</sup> , Paul Bailey <sup>2</sup> , Joshua Colmer <sup>1</sup> , Benjamen White <sup>1</sup> ,
4	Connor Reynolds <sup>1</sup> , Sabrina Jaye Ward <sup>1</sup> , Calum A. Graham <sup>3,4</sup> , Luíza Lane de Barros Dantas <sup>3</sup> ,
5	Antony N. Dodd <sup>3</sup> , Anthony Hall <sup>1</sup>
6	
7	
8	<sup>1</sup> Earlham Institute, Norwich Research Park, Norwich, NR4 7UZ, UK
9	<sup>2</sup> Royal Botanic Gardens Kew, Richmond, Surrey, TW9 3AE, UK
10	<sup>3</sup> John Innes Centre, Norwich Research Park, Norwich, NR4 7UH, UK
11	<sup>4</sup> School of Biological Sciences, University of Bristol, Bristol, BS8 1TQ, UK.
12	
13	Abstract
14	The circadian clock is a finely balanced time-keeping mechanism that coordinates
15	programmes of gene expression. It is currently unknown how the clock regulates expression
16	of homoeologous genes in polyploids. Here, we generate a high-resolution time-course
17	dataset to investigate the circadian balance between sets of three homoeologous genes (triads)
18	from hexaploid bread wheat. We find a large proportion of circadian triads exhibit
19	imbalanced rhythmic expression patterns, with no specific sub-genome favoured. In wheat,
20	period lengths of rhythmic transcripts are found to be longer and have a higher level of
21	variance than in other plant species. Expression of transcripts associated with circadian
22	controlled biological processes are largely conserved between wheat and Arabidopsis,
23	however striking differences are seen in agriculturally critical processes such as starch
24	metabolism. Together, this work highlights the ongoing selection for balance versus
25	diversification in circadian homoeologs, and identifies clock-controlled pathways that might
26	provide important targets for future wheat breeding.
27	Introduction
28	Circadian clock homologs have been both inadvertently selected during crop domestication
29	and identified as crop improvement targets <sup>1-4</sup> . Understanding circadian regulation of the

30 transcriptome in crops such as bread wheat (*Triticum aestivum*) may provide useful insights

31 for future crop improvement. Wheat also provides an excellent model system to explore how

32 the circadian clock and its outputs are co-ordinated in a recently formed, complex

33 allopolyploid. In Arabidopsis, circadian transcription factors act in a dose-dependent manner, 34 with both knock-out and over-expression mutants resulting in altered function of the circadian oscillator<sup>5–8</sup>. It is not yet understood how rhythmic gene expression is balanced in 35 36 species with multiple copies of the same gene. T. aestivum is a hexaploid (AABBDD) formed 37 through interspecific hybridisation of three diploid ancestors around 10,000 years ago<sup>9,10</sup>. 38 51.7% of high-confidence wheat genes still exist in triads; sets of three homoeologous genes 39 present on each of the A, B and D genomes<sup>11</sup>. As these homoeologs evolved independently 40 for several million years prior to hybridization, it is plausible that these independent species 41 might have been subject to different selective pressures on their clocks (Fig. 1a). 42 The circadian network in Arabidopsis comprises a series of interlocking negative transcriptional feedback loops connected by key activators<sup>12</sup>. Although monocots such as 43 wheat diverged from their dicot relatives over 140 million years ago<sup>13</sup>, many circadian 44 oscillator components seem to have been conserved, particularly those forming the core loop 45 46 network. Orthologs of TIMING OF CAB EXPRESSION 1 (TOC1) and other PSEUDO-RESPONSE REGULATOR (PRR) genes have been identified in wheat, rice and barley, and 47 several loci within these genes have been associated with altered flowering times, most 48 notably (*ppd-1*) within  $TaPRR3/7^{14-16}$ . Likewise, mutants of orthologs of *LATE* 49 ELONGATED HYPOCOTYL (LHY), GIGANTEA (GI), EARLY FLOWERING 3 (ELF3), and 50 51 LUX ARRYTHMO (LUX) have been identified that alter heading dates, pathogen 52 susceptibility, plant height or lower grain yields<sup>17–21</sup>. 53 Circadian control of carbon fixation and starch metabolism are thought to form part of the selective advantage conferred by the clock<sup>22,23</sup>. This is apparent in the *lhy<sup>-</sup>/cca1*<sup>-</sup> short period 54 double mutant, where night-time starch levels reach exhaustion earlier compared to wild-55 56 type, triggering early onset starvation responses that reduce plant productivity<sup>23</sup>. Similarly, 57 genes encoding photosynthesis-related proteins are well-established targets of the circadian 58 clock and include the LIGHT HARVESTING CHLOROPHYLL A/B BINDING PROTEIN 59 genes (*LHCB* also known as *CAB* genes) and photosystem I and II reaction centre genes<sup>24,25</sup>. 60 Here, we investigate circadian balance within wheat triads to understand how circadian 61 control is co-ordinated in a polyploid crop with three subgenomes. Second, we examine similarities and differences between the circadian transcriptome in wheat and its distant dicot 62 63 relative Arabidopsis, at a global level and at the level of genes encoding key pathways such 64 as primary metabolism and photosynthesis.

### 65 <u>Results</u>

## 66 Global analysis of the circadian transcriptome in wheat

67 We generated a circadian RNA-seq time-course and compared it with a recently published dataset from Arabidopsis<sup>26</sup> over 24h - 68h following transfer to constant light. Rhythmicity 68 69 was assessed using Metacycle Benjamini-Hochberg (BH) q-values. Of the 86,567 genes 70 expressed in wheat, 33.0% were rhythmically expressed with a BH q < 0.05 and 21.5% with 71 a BH q < 0.01 (Supplementary Note 1, Supplementary Table 1). This was significantly lower 72 than the proportions of rhythmically expressed genes in the Arabidopsis dataset (50.7% BH q < 0.05, 39.1% BH q < 0.01) using the same criteria (X<sup>2</sup> (1) = 2727.1, p < 0.001, one-tailed, 73 two-proportions z-test). Circadian waveform characteristics of the rhythmically expressed 74 75 genes (BH q < 0.01) in the wheat and *Arabidopsis* datasets were quantified using algorithms in Metacycle (JTK, ARSER, LS and meta2d) and Biodare2 (FFT-NLLS and MESA). Period, 76 77 phase, and amplitude estimates from FFT-NLLS and meta2d were well-correlated for 78 individual genes (Supplementary Fig. 1). All models reported that mean period length in 79 wheat was approximately 3h longer than in *Arabidopsis* (wheat = 25.9 - 27.5h, 80 *Arabidopsis* = 22.6 - 24.4h; t(36067) = 101.58, p<0.001, Welch's two sample t-test; 81 Supplementary Fig. 2). There was no significant difference between mean periods across the 82 three wheat sub-genomes (Fig. 1c, F(2, 28, 276) = 0.179, p=0.836, One-way ANOVA). 83 We used meta2d to compare period means and distributions from four previously published 84 circadian datasets, and found that period lengths in wheat were longer and had higher 85 standard deviation than period distributions from Arabidopsis, Brassica rapa, Brachypodium 86 distachyon and Glycine max (Fig 1b; Supplementary Table 2). We investigated how wheat periods changed over the course of the three-day experiment and 87 88 found that periods were longer immediately after transfer to constant light (28.61h, 89 SD=3.421h), and progressively shortened over the following days (Supplementary Note 2). 90 One explanation for this initial lengthening of period is that the dusk zeitgeber is an important 91 signaling cue for wheat circadian expression. It is possible that the mean period of expressed

92 transcripts initially lengthens trying to follow this missing dark signal before the free-running

- 93 endogenous period asserts itself.
- 94 For both Arabidopsis and wheat, we recalculated phases of rhythmic transcripts relative to
- 95 endogenous period (circadian time; CT). Across all algorithms, most transcripts in
- 96 Arabidopsis peaked during the subjective night (around CT12-24; Supplementary Fig. 3). In

97 wheat, the greatest numbers of rhythmic genes peaked during the subjective day (around

98 CT6-8) with a second, smaller group being expressed in the night (~CT20). When we

- 99 grouped transcripts into 2h period bins, we found that transcripts with short periods contained
- 100 proportionally more dawn-peaking transcripts, whereas those with longer periods contained
- 101 proportionally more dusk-peaking transcripts (Supplementary Note 3, Supplementary Fig. 4).

#### 102 Balance of circadian regulation within triads

103 Although previous studies have examined the relationships between circadian regulated

104 orthologs in different plant species<sup>26-28</sup> and within paralogs in *Brassica rapa*<sup>29</sup>, hexaploid

105 wheat provides an opportunity to study the relationships between recently formed circadian

106 regulated homoeologs acting within the same organism. In wheat, over 72% of syntenic triads

107 are estimated to have "balanced" expression, with similar relative abundance of transcripts

108 from each of the three homoeologs $^{30}$ . Due to the importance of the clock in coordinating

109 dosage of gene expression, our hypothesis was that many circadian triads would also have

- 110 balanced circadian regulation. We defined imbalanced circadian regulation as triads
- harbouring differences in rhythmicity (i.e., BH *q*-values), period lengths, phases, and relative
  amplitudes.

113 Of the 16,359 expressed triads in our dataset, 9901 (60.52%) had at least one rhythmic

homoeolog, and 3448 (21.08%) had three rhythmically expressed genes (BH q < 0.05), with

the latter hereafter termed "rhythmic triads" (purple segment, Fig. 1d). 6453 triads lacked

116 rhythmicity in either one or two expressed homoeolog(s) (green and blue segments, Fig. 1d).

117 In both cases, there was no bias for absence of rhythmicity in the A, B or D copy ( $\chi^2(2)$ =

118 6.8415, p = 0.40 where one gene is arrhythmic,  $\chi^2(2) = 6.8415$ , p = 0.03 where two genes are

119 arrhythmic). We found cases where high-confidence rhythmic homoeologs (BH q < 0.01)

120 occurred alongside arrhythmic homoeologs (BH q > 0.05) represented by light-shaded outer-

ring segments in Fig. 1d. In total there were 3450 of these imbalanced-rhythmicity triads

122 (Fig. 1h,i). To explore other forms of circadian imbalance, we assessed whether phase, period

123 and relative amplitude were conserved between homoeologs within the rhythmic triad set

- 124 (purple segment, Fig. 1d). Differences in phases were quantified by a cross-correlation
- 125 analysis to assess whether the correlation between homoeologs was improved with a time lag
- 126 of 4, 8 or 12 hours. We identified 464 triads with imbalanced phases with an optimum lag of
- 127 >0h between homoeologs (Fig. 1e,j). 1,139 triads had imbalanced periods with more than 2h

128 difference in period between homoeologs (Fig. 1f,k). 701 triads had imbalanced relative

amplitudes with more than two-fold difference in relative amplitude (Fig. 1g,l). Within this

130 last group, the homoeolog with the lowest amplitude was still rhythmic, as observed when

131 data are mean-normalized (Fig. 11,m). In summary, the largest cause of imbalanced circadian

- 132 expression within triads was absence of rhythmicity (67.89%) with differences in period
- 133 (22.41%), relative amplitude (13.79%) and phase (9.13%) occurring more infrequently and

134 with some overlap between categories.

135 Out of all expressed triads in our dataset, around 11.1% had balanced circadian expression,

136 31.1% had imbalanced circadian expression, 39.5% were arrhythmic and 18.4% were

- 137 borderline triads which did not fit into the categories imposed by our cut-offs. There is
- 138 therefore a ratio of approximately 3:1 imbalanced to balanced circadian triads in wheat. This

139 finding was initially surprising given that Ramírez-González et al. reported 72.5% of wheat

140 triads showed balanced expression. We found that 64.15% of the triads classified as circadian

- 141 imbalanced in our data would be classified as balanced in the Ramírez-González study
- 142 (Supplementary Fig. 5). However, if we consider that triads with highly imbalanced circadian
- 143 regulation can be classified as balanced in their expression at a single timepoint (as

144 demonstrated in Supplementary Fig. 6), and that there are multiple ways in which homeologs

145 can become circadian imbalanced (phase, period, rhythmicity etc.), then it is quite reasonable

146 that only a small proportion of triads are classified as having balanced circadian regulation in

147 this study. This insight highlights the importance of considering temporal dynamics when

148 studying gene expression.

149 One explanation for imbalanced rhythmicity is that arrhythmic homoeologs are silenced. In

150 support of this, we found that the rhythmic homoeologs in imbalanced triads were expressed

151 at a significantly higher baseline level than their arrhythmic homoeologs (Fig. 1n; F(16,

152 35,148) = 6.94, p<0.001, Two-level, nested ANOVA on Log10 transformed data). We also

153 found that triads with balanced rhythmicity were expressed at a uniformly higher level than

154 the most highly expressed homoeolog(s) in the imbalanced triads (Fig. 1n; F(7, 35, 148) =

155 570.909, p<0.001). Therefore, in imbalanced rhythmicity triads, the rhythmic homoeolog

156 does not appear to compensate for reduced expression of the other homoeolog(s), so the

157 overall expression across the triad is reduced. This is supported by data from diploid *Brassica* 

*rapa*, where circadian regulated paralogs are expressed at a higher level than single copy

159 genes<sup>29</sup>.

160 To investigate whether certain biological processes were associated with circadian balance,

161 we compared GO-slim terms enriched in the 1816 circadian balanced triads, the 5082

162 differently circadian regulated triads and the 6458 arrhythmic triads, identifying significant

163 terms unique to each group (Table 2). Some terms were enriched only in circadian balanced

- 164 triads (*p*-value <0.0001, Fisher's exact test e.g., "photosynthesis", "generation of precursor
- 165 metabolites and energy", "gene-expression" and "translation"). In contrast, GO-slim terms:
- 166 "developmental process involved in reproduction", "and "system development" were
- 167 enriched significantly in triads with differently regulated homoeologs (*p*-value <0.0001) but
- 168 not in triads with circadian balanced homoeologs (*p*-value >0.5). A possible explanation for
- 169 this enrichment could be that imbalanced circadian triads are more likely to be dynamically
- 170 expressed over developmental stages or show local dominance of a sub-genome in a
- 171 particular tissue type. Transcription factor (TF) triads were as likely to be circadian
- balanced/imbalanced as non-transcription factors ( $\chi^2$  (2, N = 13,356) = 3.03, p = 0.08, chi-
- 173 square test). Previously validated wheat TFs with imbalanced circadian expression included
- 174 *WCBF2* (aka *TaCBF1*) and *TaPCF5*, both of which regulate abiotic stress responses<sup>31,32</sup>
- 175 (Supplementary Note 4, Supplementary Fig. 7).
- 176 When we compared GO-slim terms associated with paralogs in *Brassica rapa*<sup>29</sup>, we found
- 177 that *Brassica* paralogs with similar circadian expression patterns (as characterized in
- 178 Greenham et al, (2020) using DiPALM<sup>29</sup>) were also associated with "photosynthesis" and
- 179 "generation of precursor metabolites and energy" (*p*-value <0.001, Fisher's exact test). These
- 180 terms were not enriched in circadian paralogs with differential expression patterns (*p*-value
- 181 >0.5; Supplementary Table 3). Examples of genes having similar (balanced) circadian
- 182 expression within *Brassica rapa* paralogs and in all three homoeologs in wheat triads
- 183 included orthologs of the PSI light harvesting complex genes LHCA1, LHCA2 and LHCA3,
- and the RNA polymerase sigma factor *SIG5*. It is possible that conservation of circadian
- 185 expression of these duplicate genes poses an evolutionary benefit, as similar regulation has
- 186 been retained for both duplicate copies in ancient paralogs of *Brassica rapa* and within more
- 187 recently formed wheat homoeologs arising through polyploidization.
- 188

# 189 Patterns of triad circadian balance across the genome

- 190 Next, we wanted to determine whether there are genomic regions that incorporate a clustering
- 191 of circadian balance in rhythmicity. We hypothesized that if we found sequential "runs" of
- 192 triads with arrhythmic expression on a particular chromosome, this might indicate an
- 193 overlying region of differential chromatin accessibility or transcriptional suppression. To
- 194 investigate this, we looked for regions on each set of chromosomes where there were
- 195 sequential triads having the same number of rhythmic homeologs (i.e. runs of three, two or
- 196 one rhythmic genes). We also looked for runs of sequential rhythmic triads specific to a
- 197 particular chromosome (e.g. runs of two rhythmic genes on chromosomes A and B). In both

- 198 cases, we found no evidence that triads with specific categories of rhythmic homoeologs
- 199 were grouped together more often than would be expected by chance (Supplementary Note 5,
- 200 Supplementary Table 4). This suggests that distributions of rhythmic balance appear to be
- 201 randomly distributed across the genome (Supplementary Fig. 8).
- 202

## 203 Clustering of gene expression and GO-term enrichment

- 204 To establish whether similar phased transcripts in wheat and *Arabidopsis* had similar
- biological roles, we clustered rhythmic transcripts (BH q < 0.01) into 9 expression modules
- for each species and identified GO-slim terms enriched in each module (p < 0.01). Circadian
- 207 characteristics of module eigengenes are shown in Supplementary Table 6. We compared the
- 208 correlation and cross-correlation of pairwise modules in the two species to find modules that
- 209 correlated with a peak lag of 0 (synchronous phase) or with a peak lag of 4, 8, or 12h
- 210 (asynchronous phase). Overall, modules with synchronous phases in wheat and Arabidopsis
- shared more GO-slim terms than modules with asynchronous phases (F(3,77) = 4.79, p
- 212 <0.01, One-Way ANOVA), indicating that these modules in wheat and *Arabidopsis* contain
- 213 genes with similar functions (Supplementary Fig. 9). We focused on four of these
- synchronous module pairs, broadly peaking at dawn, midday, dusk, and night for further
- analysis (Fig. 2). Eigengenes for dawn peaking modules A9 and W9 were highly correlated
- 216 (r>0.9) and shared 14 overlapping enriched GO-slim terms (p < 0.01; Fig. 2a,b,f). These
- 217 included terms for translation and gene expression as well as terms related to protein, amide,
- 218 nitrogen and organonitrogen biosynthetic and metabolic processes (full lists in
- 219 Supplementary Table 7). Co-expressed genes in the dawn-expressed modules included
- several orthologs involved in light, heat, and biological defence, as well as 45 ribosomal
- 221 protein orthologs (Supplementary Note 6). Transcripts for ribosomal proteins in mouse liver
- and *Neurospora crassa* have also been reported to oscillate, suggesting a conserved role for
- 223 the circadian clock in co-ordinating ribosome biogenesis $^{33,34}$ .
- 224 In addition to enriched GO-slim terms, we investigated enrichment for transcription factor
- 225 (TF) superfamilies and transcription factor binding sites in each wheat module of clock-
- regulated genes. In late-night/dawn modules W8 and W9, transcripts encoding MYB
- 227 transcription factors were significantly enriched and included putative TFs involved in leaf
- 228 morphogenesis, plant growth, regulation of flavonoid biosynthesis, and developmental
- transition to flowering (Supplementary Note 6, Supplementary Fig. 10).

Eigengenes for wheat and *Arabidopsis* modules peaking in the day (W3 and A2) had a relatively low correlation (*r*=0.491), but peaked with similar CT values (CT 6.34h and

- 6.19h) given the longer circadian period in wheat. 5 out of 15 of the GO-slim terms enriched
- in the W3 module were also found in the A2 module (p < 0.01; yellow triangles in Fig.
- 234 2a,c,f). These included terms relating to "photosynthesis", "response to radiation" and
- 235 "generation of precursor metabolites and energy". Co-expressed genes peaking in day-time
- 236 modules included light-harvesting and light signaling genes as well as CYP709B3, which
- 237 protects the plant from transpiration-triggered salinity stress during the day  $^{35,36}$ .
- 238 In dusk-peaking modules A5 and W4, 8 significantly enriched GO-slim terms were shared
- between Arabidopsis and wheat (p < 0.01, green triangles in Fig. 2a,d,f). Several genes co-
- 240 expressed in these dusk modules were involved in auxin transport and signalling including
- 241 the endosomal sorting complex protein *CHMP1A* which ensures proper sorting of auxin
- 242 carriers (Supplementary Note 6)<sup>37</sup>. There was also a significant enrichment for expression of
- transcripts encoding AP2-EREBP (ethylene responsive) and ARF (auxin responsive)
- transcription factor superfamilies within the W4 module (Supplementary Fig. 10).
- 245 Interestingly, this was followed two hours later by the expression of genes with AP2-EREBP
- transcription factor binding sites in their promoter region (W5, Supplementary Fig 11).
- Finally, two evening-phased modules W5 and A6 (*r*=0.80) were enriched for GO-slim terms
- 248 concerning several metabolic processes (blue triangles in Fig. 2f). Co-expressed orthologs in
- 249 these two modules included SEVEN IN ABSENTIA2 that regulates ABA-mediated stomatal
- 250 closure and drought tolerance in *Arabidopsis*<sup>38</sup>, and *HYDROPEROXIDE LYASE1* that
- 251 contributes to responses to insect attack and mechanical wounding<sup>39</sup>.
- 252 Components of the core circadian clock in Arabidopsis and wheat
- 253 We next compared the dynamics of circadian oscillator components in wheat and
- 254 Arabidopsis. Clock gene orthologs belonging to large gene families were detected by
- 255 phylogenetic analysis (Supplementary Fig. 12–16; Supplementary Table 8). Overall, wheat
- 256 circadian clock genes were expressed rhythmically and with a similar phase to their
- 257 Arabidopsis counterparts (Fig. 3). However, the free-running rhythms of clock transcripts in
- wheat had a mean circadian period that was approximately 3.49h longer than in Arabidopsis
- 259 (27.23h and 23.74h, respectively).
- 260 *TaLHY* and *TaTOC1* peaked sharply at dawn and dusk, respectively, during the first cycle in
- 261 constant light, and maintained an >8h difference in phase throughout the experiment (Fig.
- 262 3a,b). This is consistent with their phasing in Arabidopsis. All three homoeologs for TaGI

were robustly rhythmic (BH q < 0.01) and peaked at CT7 (Fig. 3c). TaPRR73 transcripts

264 peaked approximately 5h before TaPRR37 transcripts, consistent with the phase divergence 265 of Arabidopsis PRR7 and PRR3 (Fig. 3d,e). However, wheat homoeologs TaPRR59 and 266 TaPRR95 had similar expression profiles ( $R^2=0.68$ ) peaking marginally apart at CT8 and 267 CT10, in between the peak phases of Arabidopsis PRR9 (CT5) and PRR5 (CT11) (Fig. 3f,g). Therefore, the *PRR* gene family in wheat peaks in the order of; *TaPRR73*, [*TaPRR37*, 268 269 TaPRR95, TaPRR59] in quick succession, and finally TaTOC1. This sequential pattern 270 matches the expression of PRR homologs in rice<sup>40</sup>. 271 Transcripts encoding evening complex components, LUX, ELF3 and ELF4, are circadian 272 regulated in Arabidopsis and peak simultaneously at dusk. Three wheat triads for LUX-like 273 genes were identified; one with higher identity to LUX/BOA and two similar to other LUX-274 like Arabidopsis genes (Supplementary Fig. 15). Transcripts from all three of these triads 275 accumulated rhythmically and peaked from midday to dusk, TaLUX-Lb at CT7, TaLUX/BOA at CT10 and TaLUX-La at CT12 (Fig. 3h,i; Supplementary Fig. 17). Five wheat transcripts 276

278 phase of 12.6h; similar to *ELF4*, but with lower relative amplitudes (Fig. 3j,k; Supplementary

with homology to Arabidopsis ELF4 and ELF4-L1-4 accumulated with a mean circadian

- Fig. 17). *TaELF3* transcripts were all arrhythmic (BH q > 0.36), and the *TaELF3-1D*
- 280 homoeolog was expressed with a particularly low baseline level of 0.73 TPM in comparison
- to the other two homoeologs (8.7-9.7 TPM) (Fig. 31). This is consistent with previous
- findings linking a deletion in *TaELF3* to the *eps* QTL on chromosome 1D in Cadenza<sup>18</sup>.
- 283 We next assessed the balance of circadian expression between triad homoeologs in the core
- 284 clock network. TaLHY, TaGI, and TaPRR59 had notably similar expression patterns in terms
- 285 of phase, period, relative amplitudes, and baseline expression over all timepoints (Fig.
- 286 3a,c,f,g), suggesting that unbalance in these triads is strongly selected against. Homoeologs
- of *TaTOC1*, *TaPRR73* and *TaPRR37(Ppd)* had similar phases, but all had reduced expression
- in the A-genome homoeolog (Fig. 3b,d,e). *TaLUX/BOA-3A*, *TaLUX-La-3B* and *TaLUX-Lb-*
- 289 1D had marginally shorter periods (>2h) and delayed phases (>2h) compared to their
- 290 respective homoeologs (Supplementary Table 9).

263

- 291 The REVEILLE family are CCA1/LHY-like MYB-domain transcription factors that are
- 292 predominantly activators of evening expressed genes<sup>41,42</sup>. The wheat *RVE* genes could be
- split into a *LHY* clade (containing the *TaLHY* triad described above), a *RVE6/8*-like clade
- 294 containing three wheat triads and a *RVE1/2/7*-like clade also containing three triads
- 295 (Supplementary Fig. 12). All *TaRVE6/8* transcripts peaked at CT0-4 concurrently with
- 296 *TaLHY* (Supplementary Fig. 17). The *TaRVE2/7* transcripts peaked with distinct phases;

#### 297 *TaRVE27b* in phase with *TaLHY*, *TaRVE27c* 4h before *TaLHY* and *TaRVE27a*

- approximately 12h before *TaLHY* (Supplementary Fig. 17). Based on their phylogenetic
- 299 relationships, it is probable that several *RVE2/7* clade paralogs in wheat and *Arabidopsis*
- 300 arose independently after their evolutionary divergence, and it is therefore interesting that
- 301 they both show distinct phases of expression, suggesting homoplastic circadian functions.
- 302 Expression of orthologs for additional transcripts involved in circadian regulation (*FKF1*,
- 303 ZTL, LKP2, LNK1/2, CHE and LWD) are reviewed in Supplementary Note 7 and
- 304 Supplementary Fig. 17.

305 Circadian control of photosystem and light signalling gene expression is largely conserved

## 306 between Arabidopsis and wheat

307 A further GO-slim analysis across all rhythmically-expressed genes in Arabidopsis and wheat 308 identified enrichment of similar GO-slim processes including "photosynthesis" (p<1x10-14), 309 "rhythmic process" (p<1x10-6), "response to abiotic stimulus" (p<1x10-13) and "cellular 310 macromolecule biosynthetic process" (p<1x10-5, Fisher's exact test, Supplementary Table 311 10). We used genes associated with some of these GO-slim terms as case-studies to highlight 312 similarities and differences in circadian control between the two species. Expression data and 313 Metacycle statistics for all transcripts in this analysis are in Supplementary Table 11. 314 In considering photosynthesis, we examined specifically nuclear genome-encoded 315 photosystem (PS) proteins. Transcripts encoding the PSI components LHCA1-6, the PSI 316 reaction centre subunits PSAD and PSAE and the PSII subunits LHCB1-7 were rhythmically 317 expressed in both species and had conserved phases (Supplementary Fig. 18). LHCA1-4 318 peaked towards the end of the subjective day and LHCA5 and 6 peaked during the subjective 319 night. PSAD and PSAE peaked concurrently with LHCA1-4. In both species, LHCB7 320 transcripts had lower relative amplitudes compared to other LHCB transcripts. PSB27 is a 321 protein associated transiently with the PSII complex involved in adaption to fluctuating light 322 intensities<sup>43</sup>. Transcripts for this protein peaked during the subjective day in Arabidopsis and 323 during the subjective night in wheat. 324 In considering the GO-slim term "response to abiotic stimulus", we next investigated

- 325 expression of transcripts for photoreceptors and light signalling proteins due to their
- 326 pervasive influence upon development, metabolism, and circadian timing. Although
- 327 transcripts for the UV-B photoreceptor UVR8 accumulated with a circadian rhythm in both
- 328 species, only one PHYTOCHROME ortholog (PHYA) and three CRYPTOCHROME

329 orthologs (CRY1) were rhythmic in wheat out of 18 orthologs identified (Supplementary Fig.

- 18). This contrasts with *Arabidopsis*, where *PHYA-C*, *CRY1* and *CRY2* accumulated with a
- 331 circadian rhythm.
- 332 Downstream light signalling proteins COP1 and SPA form complexes that degrade positive
- 333 regulators of photomorphogenesis (e.g. *HFR1* and *HY5*) under dark conditions<sup>44</sup>. Transcripts
- for *COP1*, *SPA4*, *HFR1* and *HY5* accumulated rhythmically and with conserved phases in
- both species (Supplementary Fig. 19). COP1/SPA4 peaked synchronously around the end of
- the subjective night. Surprisingly, given the similar role HFR1 and HY5 proteins have in
- 337 preventing hypocotyl elongation in low light, *HFR1* and *HY5* transcripts were expressed anti-
- 338 phase to each other. HY5 and HFR1 act synergistically to coordinate the photomorphogenesis
- response, although it has been suggested that their activation is regulated through
- 340 independent pathways<sup>45</sup>.
- 341 Wheat triads with identity to Arabidopsis PIN1, PIN4, PIN5, and PIF4/5 were rhythmically
- 342 expressed, alongside two triads with high similarity to rice OsPIL11 and OsPIL13 (<sup>46</sup>;
- 343 Supplementary Fig. 19). Overall, we observe that the arrhythmic accumulation of most of the
- 344 wheat PHY and CRY transcripts is not reflected in the rhythmic expression of several
- 345 downstream light signalling transcripts. This supports the notion that regulatory signals from
- 346 photoreceptors might occur at the level of protein stability and localisation rather than at the
- 347 level of transcript accumulation, as occurs for *ZTL* or *HY5* in *Arabidopsis*.
- 348 A set of proteins that link light signalling, circadian regulation and chloroplasts are the sigma
- 349 factors<sup>47</sup>. These light-responsive nuclear-encoded regulators of chloroplast transcription
- 350 guide promoter recognition and transcription initiation by plastid encoded RNA-polymerase
- 351 (PEP) on the chloroplast genome<sup>48-51</sup>. In *Arabidopsis*, *SIG1*, *3*, *4*, *5* and *6* were rhythmically
- transcribed (Supplementary Fig. 19). In wheat, all homoeologs in triads orthologous to SIG1,
- 353 SIG3 and SIG5 were also rhythmic (BH q < 0.01). Whilst the dawn phase of TaSIG5
- transcripts were similar to *AtSIG5*, *TaSIG1* transcripts were expressed over 10h earlier than
- 355 AtSIG1 (Supplementary Fig. 19). Previous research has shown that activity of AtSIG1 can be
- 356 regulated through redox-dependent phosphorylation<sup>52</sup>, and activity of all sigma factors are
- 357 likely to be subject to multiple layers of regulation in addition to circadian control of
- 358 transcript expression.
- 359

#### 360 Similarities and differences in circadian control of primary metabolism genes in Arabidopsis

# 361 and wheat

- 362 Expression profiles of genes with key roles in primary metabolism were compared in 363 Arabidopsis and wheat with a focus on enzymes that regulate trehalose 6 phosphate (Tre6P) 364 and starch metabolism (Fig. 4). Tre6P synthase (TPS) and Tre6P phosphatase (TPP) 365 participate in the synthesis and dephosphorylation of Tre6P, respectively. Tre6P is an important signalling metabolite associated with both sucrose regulation and circadian 366 regulation in Arabidopsis<sup>53–55</sup>. Tre6P also affects grain yield and drought resilience in wheat, 367 maize, and rice<sup>56</sup>. Transcripts for TPS1, 2, 6, 8, 9, 10 and 11 and TPPA, E, F, G and H were 368 expressed rhythmically in Arabidopsis (Supplementary Fig. 20). Wheat transcripts for TPS1 369 370 (the most well-characterised of the T6P synthases) were arrhythmic, however rhythmic 371 transcripts were found in triads more closely related to TPS11, 6 and 7 (Supplementary Fig. 372 20). We identified three rhythmic TPP triads in wheat, two of which were orthologous to 373 Arabidopsis TPPA, F and G. The third TPP triad was part of a monocot-specific clade
- identified by Paul et al. (2018), which also included *Zm00001d032298*, a crop improvement target in maize<sup>56</sup>.
- 376 Ribulose bisphosphate carboxylase (Rubisco) comprises eight small (RbcS) and 8 large
- 377 (RbcL) subunits, which are encoded by the nuclear and chloroplast genomes, respectively<sup>57</sup>.
- 378 Rubisco requires activation by Rubisco activase (RCA) to release its activity from inhibitory
- 379 substrates<sup>58</sup>. In our wheat expression data, 22 putative wheat orthologs for the small subunit
- 380 of Rubisco were rhythmic, peaking during the subjective night, as *RBCS1A*, *RBCS1B*,
- 381 *RBCS2B* and *RBCS3B* do in *Arabidopsis* (Supplementary Fig. 20). Two triads with identity to
- 382 Rubisco activase were identified, one of which accumulated rhythmically (peaking at CT0, as
- 383 with Arabidopsis RCA).
- 384 Circadian regulation has a pervasive influence on starch metabolism in Arabidopsis,
- 385 particularly the nocturnal rate of transitory starch degradation<sup>23,59</sup>. Chloroplast phospho-
- 386 glucose isomerase 1 (*PGII*) and chloroplast phosphoglucose mutase (*PGMI*) are essential
- enzymes that link the Calvin-Benson cycle with starch biosynthetic pathway<sup>60-62</sup>. In
- 388 *Arabidopsis*, these transcripts accumulated with a circadian rhythm (BH  $q < 1x10^{-4}$ ); *PGM1*
- peaked just after dusk (CT14), and *PGI1* slightly later at CT20. In contrast, only one wheat
- 390 *TaPGI1* homoeolog was rhythmic (BH q < 0.01), which had a low relative amplitude (0.16)
- and a peak phase of CT8. No homoeologs for TaPGMI were rhythmically expressed (BH q >
- 392 0.01, Supplementary Fig. 20).

393 ADP-glucose pyrophosphorylase (AGPase) mediates the first irreversible and rate-limiting 394 step in starch biosynthesis through the formation of ADP-Glc. In Arabidopsis, transcripts 395 encoding the small and large subunits of AGPase (APL1, APL2, APL3, APS1) were rhythmic, 396 peaking at night around CT20. In comparison, in wheat only two of the eleven transcripts 397 with homology to APL1, APL2 and APS1 were rhythmic (BH q < 0.01), with the remaining 398 transcripts lacking a discernible rhythm (BH q > 0.05) (Supplementary Fig. 20). 399 Starch synthases (SS) represent another group of metabolically important enzymes that use 400 the glucose from ADP-Glc to elongate glucan chains. In Arabidopsis, there are five types: 401 SSI, SSII, SSIII, SSIV and granule bound GBSSI. SSI-IV are responsible for synthesis of 402 amylopectin, with SSIII and IV determining starch granule number and morphology<sup>63</sup>. GBSSI 403 is a known dawn-expressed gene, regulated directly by CCA1/LHY, specialised for amylose synthesis<sup>64</sup>. In wheat, *GBSSI* orthologs are called *TaWaxy* and cultivars with three null alleles 404 produce amylose-free starch in their grain<sup>65</sup>. Comparison of starch synthase expression in 405 406 Arabidopsis and wheat revealed several differences between the phases and relative 407 amplitudes of these transcripts (Supplementary Fig. 20). In Arabidopsis, GBSSI transcripts 408 had by far the greatest relative amplitude (1.26) with peak expression at dawn. The next 409 greatest amplitudes were of SSIV transcripts, which peaked at CT17. SSII and SSIII peaked 410 together at CT21 and SS1 peaked at CT8 with a much smaller amplitude (0.12). In contrast, 411 in wheat, an SSIII triad (TaSSIIIb) had the largest relative amplitude rhythms of the wheat 412 starch synthases identified (0.64 - 0.73). Wheat transcripts for SSI and SSIV also peaked in 413 the morning, whereas wheat SSII peaked instead in the subjective night (~CT15). In our data, 414 TaWaxy (GBSSI) transcripts were present at a very low baseline level (<0.01 TPM) and without any circadian oscillation. However, another wheat triad, TaGBSSII, shared >62% 415 416 identity with Arabidopsis GBSSI, and the B and D homoeologs had rhythmic expression 417 which peaked at dawn. TaWaxy and *TaGBSSII* are specific to endosperm and leaf tissues, 418 respectively<sup>66</sup>, which might explain the distribution of transcript accumulation seen here. We 419 can conclude that the circadian clock regulates the expression of SS transcripts in both 420 Arabidopsis and wheat, although there might be an emphasis on different types of SS in each 421 species. 422 The Arabidopsis circadian clock regulates the rate of starch degradation so that starch reserves are depleted precisely at subjective dawn<sup>23</sup>. Many transcripts encoding starch-423

- 424 degrading enzymes in Arabidopsis had synchronized dusk peaks: Isoamylase-type starch
- 425 debranching enzyme *ISA3*; alpha-amylase *AMY3*; plastidial phosphorylase *PHS1-2*;
- 426 disproportionating enzymes DPE1-2; glucan, water dikinases GWD1 and PWD and glucan

phosphatase *SEX4. Arabidopsis* transcripts for *BAM3*, *BAM5* and *PU1* also oscillated with a
circadian rhythm, peaking later in the subjective night. Strikingly, wheat orthologs for several
of these genes were not rhythmic, including *AMY3*, *DPE1*, *PWD*, *PHS1*, *PU1* and *BAM1*.
Wheat orthologs for *ISA3* and *DPE2* were expressed rhythmically, but peaked approximately
8-12 h ahead of their *Arabidopsis* counterparts. Some starch degradation enzymes had

432 conserved circadian expression patterns in the two species, such as SEX4, GWD1, BAM3 and

433 BAM5 transcripts. GWD catalyses glucan phosphorylation and SEX4 encodes a

434 phosphoglucan phosphatase, both of which facilitate hydrolytic attack by  $\beta$ -amylases (BAM)

435 in the early steps of starch degradation  $^{59,67}$ .

436

### 437 <u>Discussion</u>

# 438 <u>Conservation of circadian regulation between homoeologous genes</u>

We identified a large proportion of imbalanced circadian triads in our dataset. It was ourinitial expectation that there would be strict balance between the majority of circadian

441 regulated homoeologs due to the critical and finely balanced role the clock has in regulating

the transcriptome, and due to the reported high levels of balance reported from single-

443 timepoint transcriptomic analysis in wheat<sup>30</sup>. Instead, we find three times as many triads with

444 imbalanced circadian rhythms as triads with balanced circadian rhythms. This is likely to be

445 partly due to our multiple classification of circadian imbalance as any triad with different

446 rhythmicity, period, phase or relative amplitudes between homeologs. Another factor which

447 distinguishes ratios of transcriptional balance (as defined by Ramírez-González et al. (2018))

448 and circadian balance is that transcriptional balance within circadian triads is often dynamic

449 across a time-course, shifting between balanced, dominant and supressed relationships over

450 time (Supplementary Fig 6).

451 Most of these imbalanced circadian triads were imbalanced due to arrhythmicity in one or

452 two homoeologs expressed at a lower mean level than the rhythmic homeologs. The

453 reduction of expression could be due to constitutive epigenetic silencing or changes to

454 promoter regions, allowing differential binding of transcription factors<sup>68–70</sup>. These are likely

455 to be triads where one or two homeologs take responsibility for performing the biological

456 function of the triad, and the other homoeolog has reduced functionality. We found additional

457 circadian unbalance in the form of altered phase, period, and relative amplitudes. It is

458 possible that some of these differences are due to retention of circadian regulation from the

ancestral genome of each homeolog (Fig. 1a), although it is likely that other differences

460 reflect more recent diversification in expression as a step towards neo-functionalisation. It

461 has been previously suggested that functional divergence is a likely fate for duplicated genes

462 in a sufficiently large population<sup>71</sup>. In *B. rapa*, 42% of circadian controlled paralogs had

463 differential expression patterns<sup>29</sup>, however these paralogs arose through whole genome

464 duplication events around 13-43 million years ago, so have been exposed to longer periods of

465 time during which selection could act upon these duplicate genes<sup>72</sup>. In comparison,

466 specialisation of circadian homeologs in wheat could be comparatively lower due to the

467 relative infancy of its polyploidisation around 10,000 years ago.

468

#### 469 <u>Differences between periods of rhythmic transcripts in Arabidopsis and wheat</u>

470 The mean period of circadian regulated genes in wheat was over three hours longer than in Arabidopsis. Period length is affected by a range of exogenous conditions (e.g. light and 471 temperature), and varies between tissues and plant age<sup>73</sup>. There is also evidence that longer 472 473 periods have been selected for during cultivation of crops at higher latitudes<sup>1,2,74</sup>, potentially due to enhanced seasonal tracking capability enabling precision timing of growth and 474 flowering<sup>75</sup>. Compared to other plant circadian transcriptome data sets, rhythmic wheat 475 476 transcripts also had higher period variance (Fig 1b). The broad period distribution in wheat 477 might be due to inclusion of all aerial material in our sampling strategy. Variation in free-478 running periods could occur at the organ-, tissue- or cellular-level, and transcripts which are 479 highly expressed in those regions may reflect those period differences<sup>76,77</sup>. An alternative possibility is that period variation is due to uncoupling of multiple circadian oscillators within 480 the same cell which control expression of subsets of transcripts<sup>78–80</sup>. Future research could 481 482 examine the relationship between period distributions of circadian transcriptomes and the 483 effects of domestication, latitudinal adaption, monocot-dicot divergence, or polyploidy.

484

# 485 <u>Similarities and differences in circadian regulation between wheat and Arabidopsis</u>

486 Our analysis revealed extensive conservation of time-of-day specific GO-slim processes and

487 co-expressed genes between *Arabidopsis* and wheat. These included genes involved in

488 photosynthesis (e.g., photosystem proteins), light signalling (e.g., *HFR1*, *HY5*, *PINs* etc),

- 489 translation (e.g., ribosome proteins) and auxin and ethylene responsive transcription factors.
- 490 The striking conservation of photosynthesis related genes was also reflected by the
- 491 enrichment of these genes in both balanced wheat triads and similarly expressed circadian

- 492 paralogs in *Brassica napus*. Photosynthetic outputs have also been reported to be governed
- 493 by the circadian clock in the liverwort species *Marchantia polymorpha*, in diazotrophic
- 494 cyanobacterium Cyanothece sp. and in alga Aegagropila linnaei, perhaps suggesting a
- 495 widespread control mechanism with an ancient evolutionary origin<sup>81-83</sup>.
- 496 We also identified several interesting differences between *Arabidopsis* and wheat, including
- 497 absence of rhythmicity in wheat *PHY* and *CRY* transcripts and antiphase expression of the
- 498 wheat sigma factor *SIG1*. Furthermore, we found differences in rhythmic expression of many
- 499 transcripts involved in regulating Tre6P and starch metabolism.
- 500 In our data, putative wheat homeologs of *TPS1* were arrhythmic. Instead, rhythmic *TPS*
- 501 transcripts in wheat had similarity to Arabidopsis TPS11, 6 and 7 (Supplementary Fig. 20). In
- 502 *Arabidopsis*, TPS1 is the most catalytically active and best characterised TPS, and feeds back
- 503 into the entrainment of the circadian clock<sup>54,84</sup>. If the lack of rhythmicity in wheat *TPS1*
- 504 transcripts is reflected at the level of protein activity, it may indicate that Tre6P synthesis is
- 505 not regulated as tightly by the circadian clock in wheat as in *Arabidopsis*. On the other hand,
- 506 circadian control of other TPS triads may have implications for biotic or abiotic defence in
- 507 wheat. TPS5-11 have been previously implicated in control of stomatal aperture<sup>85</sup>,
- 508 thermotolerance<sup>86</sup>, and defence against fungal, bacterial and aphid attack<sup>87,88</sup>. In rice, *OsTPS8*
- 509 influences drought resistance through suberin deposition<sup>89</sup>, and wheat *TaTPS11* participates
- 510 in a cold stress response<sup>90</sup>.
- 511 In wheat, transcripts for starch degradation enzymes (PHS1, DPE1, BAM1, PU1, AMY3,
- 512 *PWD*) and starch biosynthesis enzymes (*PGI1*, *PGM1*, *ISA1* and *ATPase*) had either
- 513 arrhythmic expression or low relative amplitudes compared with the robust rhythms of many
- 514 of these transcripts in *Arabidopsis*. Additionally, *ISA2*, *ISA3* and the starch synthases (*SSI-IV*)
- 515 had differing circadian phases between the two species. While it is possible that rhythmic
- 516 expression of a reduced number of genes (e.g.: SEX4, GWD1, BAM3 and BAM5) is sufficient
- 517 to mediate circadian control of starch degradation in wheat, these data suggest that the
- 518 circadian clock has a less pervasive influence upon transcriptional control of starch
- 519 metabolism in wheat compared to *Arabidopsis* (Supplementary Note 8).
- 520
- 521 <u>Conclusions</u>
- 522 Our data reveal the influence of circadian regulation on the wheat transcriptome and highlight
- 523 several intriguing differences between rhythmically expressed transcripts in *Arabidopsis* and
- 524 wheat. It explores the added complexity of co-ordinating circadian expression across multiple
- 525 sub-genomes in a hexaploid species. Given the circadian clock has been under selection

526 during domestication and presents multiple targets for crop improvement, it is likely that this

527 new insight into the clock in wheat will be important in the development of new sustainable

528 and resilient cultivars. It is our hope that these data provide a resource for identifying target

529 genes regulated by the circadian clock, allowing the relationships between chronotype, yield

- 530 and resilience to be explored in future studies.
- 531

#### 532 Methods

#### 533 Plant materials and growth conditions

534 Wheat: Wheat seeds of the spring wheat cv. Cadenza were imbibed for three days on damp 535 filter paper on a Petri dish at 4°C. Plates were moved at dawn (06.00 = ZT0), to a growth cabinet set to 22°C under 12:12 light: dark cycles (approximately 200 µmol m-2 s-1). After 536 537 two days, only seedlings with fully emerged radicles were sown, 3 cm deep in Petersfield 538 cereal mix in 9cm pots. Plants were not vernalized. Seedlings were grown under 539 12hlight:12hdark conditions for 14 days. After 14 days, at dawn (ZT0) seedlings were 540 transferred to constant light conditions, tissue was sampled every 4h for 3 days (18 samples 541 in total). At each timepoint, we sampled the entire aerial tissue from 3 replicate plants, which was frozen immediately in liquid nitrogen before storage at -80°C. Total RNA was extracted 542 543 using Qiagen RNeasy plant mini kits (cat. no. 74904) with on-column DNAse treatment (RNAse-Free DNase Set (cat. no. 79254). RNA concentration and integrity were quantified 544 545 using a Nanodrop Spectrophotometer and Perkin Elmer LabChip GX Nucleic acid analyser 546 before sequencing. Details of growth conditions for Arabidopsis<sup>26</sup>, Brassica rapa<sup>29</sup>, Brachypodium distachyon<sup>27</sup>

547

and Glycine max<sup>28</sup> datasets can be viewed in their source manuscripts. Briefly, all circadian 548

549 data were measured under constant light and temperature following 12h:12h light:dark

entrainment other than Glycine max<sup>28</sup> which was entrained under 16h:8h light:dark cycles. 550

551 Wheat mRNA sequencing, read alignment and quantification

Library preparation was carried out following the Illumina TruSeq protocol and reads were 552

553 sequenced on a NovaSeq S2 flow cell at the Earlham Institute. 150bp paired-end reads were

554 generated from each library to an average depth of 84M reads per replicate. Reads were

555 filtered for quality and any remaining adaptor sequence was trimmed with Trimmomatic<sup>91</sup>.

Surviving reads were aligned to the Chinese Spring RefSeq v1.1 wheat genome<sup>11</sup> using 556

557 HISAT2<sup>92</sup> with default parameters. Uniquely mapping reads were then quantified using

558 StringTie<sup>93</sup> and TPM values were extracted for each gene per sample.

- 559 Processing and quantification of previously published datasets
- 560 Raw reads from previously published circadian datasets were downloaded for *Arabidopsis*<sup>26</sup>,
- 561 *Brassica rapa*<sup>29</sup>, and *Brachypodium distachyon*<sup>27</sup>. These reads were filtered for quality, and
- 562 any remaining adaptor sequence trimmed with Trimmomatic<sup>91</sup>. Surviving reads were aligned
- using HISAT2<sup>92</sup> to *A. thaliana* genome (TAIR 10), *B. rapa* genome (v1.0) and the *B.*
- 564 *distachyon genome* (v3.0) respectively. For the *Arabidopsis* alignment, maximum intron
- 565 length was set to 5000nt consistent with pre-processing in<sup>26,94</sup>. StringTie<sup>93</sup> was used to
- 566 quantify uniquely mapping reads before TPM value extraction at gene level. For *Glycine*
- 567 max<sup>28</sup>, FPKM normalised reads were downloaded from the *Glycine max* RNA-seq Database<sup>95</sup>
- 568 (accession GSE94228) and were converted from FPKM to TPM prior to analysis.
- 569
- 570 <u>Homolog identification of circadian clock and circadian controlled genes</u>

571 Wheat homologs of *Arabidopsis* core circadian clock genes were identified in the wheat

572 genome by detecting similarity to the following conserved protein family domains that are present in the proteins encoded by these genes: MYB1R, a subtype of MYB domain that 573 574 contains a distinctive SHAQKY sequence motif (present in the CCA1, LHY and RVE[1-8]) or a distinctive SHLQKY sequence motif (present in LUX), PAS (present in ZTL), PRR 575 (present in TOC1 and PRR[3579]) and ELF4 (present in ELF4). A hidden Markov model 576 577 (HMM) for each domain was used in HMMER 3.2.1 HMMSEARCH<sup>96</sup> to search for 578 members of the domain family in the following proteome datasets: Araport11 (Arabidopsis 579 thaliana), RGAP7 (Oryza sativa), JGI Phytozome version 12 (Brachypodium distachyon), 580 IBSC (Hordeum vulgare), SpudDB PGSC v4.03 (Solanum tuberosum) and IWGSC Refseq 581 v1.1 (*Triticum aestivum*). The HMMs provided by Pfam (https://pfam.xfam.org/) were used 582 for the PAS domain (PAS 9, PF13426), the PRR domain (Response reg, PF00072) and the 583 ELF4 domain (PF07011). For the MYB domain, an HMM was built for the MYB1R 584 subfamily using HMMER3 HMMBUILD<sup>96</sup> with an alignment of protein sequences from Arabidopsis and rice, previously established as being members of this subfamily. The 585 586 sequences found from these genomes were re-aligned to the original alignment using 587 HMMER 3.2.1 HMMALIGN<sup>96</sup>. Amino acids with non-match states in the HMM were 588 removed from the alignment and alignment columns with <70% occupancy were also

589 removed. The longest splice variant of each protein was selected to estimate a phylogenetic tree with bootstrap support using RAxML 8.2.12<sup>97</sup> with the following method parameters set: 590 591 -f a, -x 12345, -p 12345, -# 100, -m PROTCATJTT. The trees were mid-point rooted and images created using the Interactive Tree of Life (iToL) tool<sup>98</sup>. For the larger MYB and PRR 592 families, proteins from the tree clades containing known clock gene(s) were re-aligned across 593 594 their full-length and a "nested" phylogenetic tree was re-estimated with RAxML as described 595 above. The tree was visualised in the Interactive Tree Of Life (iTOL) website alongside the 596 corresponding alignment. This view provided increased detail about the relationships within 597 the clade and enabled orthologous sequences to be inferred. Wheat homologues for ELF3, 598 GI, LWD1/2, CHE, and LNK1/2 were identified by BLASTP searches using previously 599 identified wheat and Brachypodium predicted proteins confirmed by reciprocal BLAST 600 searches against Arabidopsis. IDs and source references can be viewed in Supplementary 601 Table 8. 602 Putative wheat orthologs for Arabidopsis circadian controlled pathway genes involved in 603 photosynthesis, light-signalling and primary metabolism were first extracted using Biomart

004 v0.7<sup>99</sup> available from Ensembl Plants and taken forward if they had >40% identity in the

605 DNA sequence. Orthologs were then verified using BLASTP using Arabidopsis protein

606 sequences as a query against the wheat protein database to confirm the wheat gene IDs.

607 Complete lists of wheat gene IDs used in the pathway analysis can be viewed in

608 Supplementary Table 11.

609

# 610 <u>Circadian quantification using Metacycle and Biodare2</u>

611 To estimate proportions of rhythmic genes expressed in Arabidopsis and wheat, we removed 612 only genes with 0 TPM at all timepoints. This approach has been used in several previous studies<sup>26,100,101</sup> and allows detection of low-expression rhythmic transcripts. An analysis of 613 614 how filtering for low-expression genes affects the estimates of proportions of rhythmically expressed genes is discussed in Supplementary Note 1 and Supplementary Table 1. 615 616 The R package MetaCycle<sup>102</sup> was used to identify rhythmically expressed transcripts 617 (Benjamini-Hochberg q-values) and to quantify period lengths (hours), absolute phase 618 (hours), baseline expression (TPM), amplitudes (TPM) and relative amplitudes of circadian 619 waveforms. Relative amplitude is the ratio between amplitude and baseline TPM if the 620 baseline is greater than 1. Metacycle integrates results from three independent algorithms 621 (ARSER, JTK CYCLE and Lomb-Scargle) to produce summary "meta2d" statistics that

- 622 combine the outcome from these algorithms. Metacycle was run using the following
- 623 parameters; minper = 12, maxper = 35, adjustPhase = "predictedPer". Transcripts were
- defined as rhythmic if they had q-values < 0.05 and high confidence rhythmic transcripts if
- 625 they have q-values < 0.01. To calculate circadian phase (CT; relative to period length=24),
- 626 meta2d phase estimates were multiplied by 24 and then divided by the period estimates for
- 627 each transcript. Circular phase means were calculated using the package 'circular'
- 628 implemented in  $R^{103}$ .
- 629 There are many different algorithms available for quantification of rhythmicity within time-
- 630 series data, some of which perform better on datasets with higher levels of noise, non-24h
- 631 periods or various sampling frequencies. To validate the meta2d results we also used the
- 632 FFT-NLLS and MESA algorithms implemented in Biodare2 to verify our observations about
- 633 period, phase and rhythmicity<sup>104</sup>. FFT-NLLS also provides relative amplitude error (RAE)
- 634 statistics which represent a useful metric for assessing rhythmic robustness. FFT-NLLS and
- 635 MESA were run using the BH q < 0.01 filtered transcripts categorized in Metacycle, and with
- 636 the following parameters: no dtr, min-max, p(12.0-35.0).
- 637 To enable as close a comparison with the Arabidopsis dataset as possible, the wheat time-
- 638 course was cropped to a data window of 24-68h for approximation of period, phase and
- 639 relative amplitude unless specified otherwise. This data-window also ensures that
- 640 measurements are being made under circadian conditions following transfer to constant light.
- 641 For the triad analysis, meta2d estimates were measured over the full time-course (0-68h) as
- 642 differentiation of homeolog behaviour was the main interest, including the response to
- transfer to L:L.
- 644
- 645 <u>Clustering of rhythmic genes into expression modules</u>

646 Gene co-expression analysis was carried out using the R package WGCNA (Langfelder and

- 647 Horvath, 2008; R version 3.6.0.).
- 648 Arabidopsis: The 10,317 genes identified by MetaCycle as significantly rhythmic (q-value <
- 649 0.01) were filtered and genes with greater than 0.5 TPM average expression at more than
- 650 three timepoints were retained for further analysis. The average expression at each timepoint
- 651 for the remaining 10,129 genes was used to construct signed hybrid networks on a replicate
- basis using the blockwiseModules() function. The soft power threshold was calculated as 18,
- and the following parameters were used; minModuleSize = 30, corType = bicor,
- maxPOutliers = 0.05, mergeCutHeight = 0.15. Highly connected hub genes were identified

655 for each of the 9 co-expression modules using the function chooseTopHubInEachModule() 656 and eigengenes were identified for each module using the moduleEigengenes() function. 657 Wheat: The 18,633 genes identified by MetaCycle as significantly rhythmic across 12 658 timepoints ZT24 - ZT68 (q-value < 0.01) were filtered and genes with greater than 0.5 TPM 659 average expression at more than three timepoints were retained for further analysis. The average expression at each timepoint for the remaining 16,327 genes was used to construct 660 661 signed hybrid networks using the blockwiseModules() function. A soft power threshold of 18 was used, together with the following parameters; minModuleSize = 30, corType = bicor, 662 663 maxPOutliers = 0.05, mergeCutHeight = 0.15. Eigengenes were identified for each module 664 using the moduleEigengenes() function. Modules with closely correlated eigengenes were 665 merged using the mergeCloseModules() function, with the parameters; cutHeight = 0.25, iterate = F) and new module eigengenes were calculated for the resulting 9 modules. 666

667

# 668 <u>Cross-correlation analysis</u>

669 A cross-correlation analysis was used to find the shift in time (lag) which produced the 670 highest (peak) correlation between two rhythms. This approach was used to identify modules 671 which peaked synchronously (had a peak lag of 0h) or asynchronously (had a peak lag of 4, 8 672 or 12h) by correlating eigengenes for each module (Supplementary Fig. 9). We also used cross-correlation to identify imbalanced phases within rhythmic triads (Fig. 1E). Before 673 674 calculating the cross-correlation between two expression rhythms, we first scaled both 675 expression patterns using their means and standard deviations, so the output reflects a time-676 dependent Pearson correlation coefficient ranging between -1 and 1:

677 
$$Z_A = \frac{X_A - \bar{X}_A}{S_A}, Z_B = \frac{X_B - \bar{X}_B}{S_R}$$

678 Where  $Z_i, X_i, \bar{X}_i$  and  $S_i$  represent the standardised expression level, tpm expression level, 679 mean expression level, and standard deviation of gene A and B respectively. Once both 680 expression patterns have been scaled, the discrete cross-correlation between the two expression patterns is calculated using the np.correlate function and is divided by the number 681 682 of time points in the expression signal returning the Pearson correlation coefficient at 683 different lags. The index of the array with the largest Pearson correlation coefficient score 684 corresponds to the lag that maximises the phase similarity between the two temporal 685 expression patterns.

#### 686 <u>Mean-normalised data for oscillation plots</u>

687 Oscillation plots in Supplementary Fig. 18-20 were mean normalised to aid visualisation of

- 688 period and phase differences between transcripts. Data was adjusted by dividing the TPM
- 689 values at each timepoint by the mean across all timepoints for each gene so that the baseline
- 690 expression was equal to 1.

#### 691 <u>Gene ontology term enrichment</u>

- 692 Functional enrichment of differentially expressed genes for biological processes within each
- 693 module was performed using the gene ontology enrichment analysis package, top $GO^{105}$  in R
- 694 (version 3.6.0, with the following parameters: nodeSize = 10, algorithm = "parentchild",
- 695 classicFisher test p < 0.05). Enrichment of terms in all rhythmic genes in *Arabidopsis* and
- 696 wheat was compared against a background 'gene universe' of all expressed genes in each
- 697 dataset (26,392 genes for *Arabidopsis* and 86,567 for wheat). This gene universe was also
- 698 used in the GO-slim analysis for enrichment in circadian balanced versus imbalanced triads.
- 699 Enrichment of terms in expression modules was compared against a background of all
- 700 rhythmically expressed genes (BH q < 0.01) which clustered into modules in each dataset
- 701 (10,129 genes for *Arabidopsis* and 16,327 for wheat). GO-slim terms refer to ontology terms
- for biological processes unless otherwise specified and were obtained from Ensembl Plants
- 51<sup>11</sup>, using the BioMart tool. The bubble plot was plotted using ggplot in R adapting code
- 704 from De Vega et al.,  $2021^{106}$ .
- Enrichment of GO-slim terms in *B. rapa* circadian paralogs with similar and differential
- 706 expression patterns was conducted using previously published DiPALM results for pattern
- <sup>707</sup> change in a LDHC circadian time course (Supplementary File 4, Greenham et al. 2020<sup>29</sup>).
- Paralog pairs with a pattern change *p*-value of <0.001 were termed differential patterns and
- pairs with a pattern change *p*-value of >0.1 were considered to be similar patterns. In this
- analysis we ignored differences in expression change for consistency with our wheat triads.
- 711 Data was first filtered for rhythmicity using Metacycle q-values <0.01. Only paralog pairs
- 712 with two significantly rhythmic paralogs were retained for the GO-slim analysis. Enrichment
- of terms in similarly expressed circadian paralogs (1562 genes) or differentially expressed
- 714 paralogs (1438 genes) in B. napus was compared against a background of 4646 genes
- 715 expressed in the Greenham dataset in paralogs and which had GO-slim annotation available.
- 716
- 717

## 718 Enrichment analysis of transcription factor superfamilies in wheat co-expression modules

719 Genes annotated as members of transcription factor superfamilies<sup>30</sup> were identified in each

720 co-expression module and the frequency of each TF superfamily compared to the frequency

721 observed in the 16,327 genes submitted to WGCNA. TF families were classed as either

- significantly under or overrepresented in each module using Fisher's exact test ( $p \le 0.05$ ).
- 723

#### 724 Enrichment analysis of transcription factor binding sites in wheat co-expression modules

725 1.5 kb of sequence upstream of the transcription start site (TSS) was extracted for each of the 726 16,327 genes submitted to WGCNA. FIMO, from the MEME tool suite (v 4.11.1) was used 727 to predict TFBS in these regions based on similarity with previously DAP-seq validated 728 TFBS identified in Arabidopsis<sup>107</sup>. FIMO was run as reported in Ramírez-González et al., 2018 (p-value threshold of <1e-04 (default), --motifpseudo set to 1e-08 as recommended for 729 730 use with PWMs and a --max-stored-scores of 1,000,000). The background model was 731 generated from the 16,327 promoter sequences using MEME fasta-get-markov. As the 732 significance of multiple matches of a single TFBS family in the putative promoter region for 733 each gene is unknown, we derived a non-redundant (nr) list of matched TFBS motifs for each 734 gene within each of the nine modules and for the complete set of 16,327 genes, where 735 multiple occurrences of a TFBS superfamily in a single promoter sequence were only counted once. The frequency of these nrTFBS motifs for each co-expression module was 736 737 compared to the frequency of nrTFBS seen across all 16,327 genes and families significantly 738 under or overrepresented in each module were identified using Fisher's exact test ( $p \le 0.05$ ). 739

### 740 <u>Loom plots</u>

741 Genome position data for the plots are based on annotations from Chinese spring

742 (Triticum\_aestivum.IWGSC.52.gtf) downloaded from Ensembl Plants. Code for creating

743 Loom plots (Supplementary Fig 8) is implemented in R and a code package with

accompanying R markdown notebooks is available from our groups GitHub repository

745 (https://github.com/AHallLab/triad.expression).

## 746 <u>Statistical analysis</u>

- 747 Statistical tests including Welch's two sample t-test, Two-proportions z-test, One-way
- ANOVA, Two-level, nested ANOVA and Chi-square tests of independence were all
- conducted in the R 'stats' package (version 4.0.0) with default parameters.
- 750

751 Data availability

- 752 Fastq data from the RNA-seq circadian time course are available to view from the Grassroots
- 753 Data Repository: <u>https://opendata.earlham.ac.uk/opendata/data/wheat\_circadian\_Rees\_2021</u>.
- 754 [Data will be uploaded to the European Nucleotide Archive (ENA) during the review
- 755 process] A summary csv table with expression of wheat genes (TPM), Metacycle estimates,
- gene annotations and triad balance classification can be viewed in Supplementary Table 12
- also available here:
- 758 <u>https://opendata.earlham.ac.uk/opendata/data/wheat\_circadian\_Rees\_2021</u>.
- 759

# 760 <u>References</u>

- Greenham, K. *et al.* Geographic variation of plant circadian clock function in natural and agricultural
   settings. *J. Biol. Rhythms* **32**, 26–34 (2017).
- 763 2. Müller, N. A. *et al.* Domestication selected for deceleration of the circadian clock in cultivated tomato.
  764 *Nat. Genet.* 48, 89–93 (2016).
- 765 3. McClung, C. R. Circadian Clock Components Offer Targets for Crop Domestication and Improvement.
  766 *Genes (Basel).* 12, 374 (2021).
- 567 4. Steed, G., Ramirez, D. C., Hannah, M. A. & Webb, A. A. R. Chronoculture, harnessing the circadian
  clock to improve crop yield and sustainability. *Science (80-. ).* 372, (2021).
- 769 5. Hazen, S. P. *et al.* LUX ARRHYTHMO encodes a Myb domain protein essential for circadian rhythms.
  770 *Proc. Natl. Acad. Sci. U. S. A.* 102, 10387–10392 (2005).
- Nakamichi, N., Kita, M., Ito, S., Yamashino, T. & Mizuno, T. PSEUDO-RESPONSE REGULATORS,
  PRR9, PRR7 and PRR5, Together play essential roles close to the circadian clock of Arabidopsis
  thaliana. *Plant Cell Physiol.* 46, 686–698 (2005).
- 774 7. Somers, D. E., Webb, A. A. R., Pearson, M. & Kay, S. A. The short-period mutant, toc1-1, alters
  775 circadian clock regulation of multiple outputs throughout development in Arabidopsis thaliana.
  776 Development 125, 485–494 (1998).
- 8. Wang, Z. Y. & Tobin, E. M. Constitutive expression of the CIRCADIAN CLOCK ASSOCIATED 1
- 778 (CCA1) gene disrupts circadian rhythms and suppresses its own expression. *Cell* **93**, 1207–1217 (1998).
- Salamini, F., Özkan, H., Brandolini, A., Schäfer-Pregl, R. & Martin, W. Genetics and geography of wild
  cereal domestication in the near east. *Nature Reviews Genetics* vol. 3 429–441 (2002).
- 10. Araus, J. L., Slafer, G. A., Romagosa, I. & Molist, M. FOCUS: Estimated wheat yields during the

782		emergence of agriculture based on the carbon isotope discrimination of grains: Evidence from a 10th
783		millenuim BP site on the euphrates. J. Archaeol. Sci. 28, 341-350 (2001).
784	11.	IWGSC et al. Shifting the limits in wheat research and breeding using a fully annotated reference
785		genome. Science (80 ). 361, (2018).
786	12.	Hernando, C. E., Romanowski, A. & Yanovsky, M. J. Transcriptional and post-transcriptional control of
787		the plant circadian gene regulatory network. Biochim. Biophys. Acta - Gene Regul. Mech. 1860, 84-94
788		(2017).
789	13.	Chaw, S. M., Chang, C. C., Chen, H. L. & Li, W. H. Dating the monocot-dicot divergence and the
790		origin of core eudicots using whole chloroplast genomes. J. Mol. Evol. 58, 424-441 (2004).
791	14.	Turner, A., Beales, J., Faure, S., Dunford, R. P. & Laurie, D. A. The pseudo-response regulator Ppd-H1
792		provides adaptation to photoperiod in barley. Science (80 ). 310, 1031-1034 (2005).
793	15.	Shaw, L. M., Turner, A. S. & Laurie, D. A. The impact of photoperiod insensitive Ppd-1a mutations on
794		the photoperiod pathway across the three genomes of hexaploid wheat (Triticum aestivum). Plant J. 71,
795		71–84 (2012).
796	16.	Laurie, D. A. Comparative genetics of flowering time. Plant Mol. Biol. 35, 167-177 (1997).
797	17.	Xiang, Y. Z., Mao, S. L., Jia, R. L., Chun, M. G. & Xian, S. Z. The wheat TaGI1, involved in
798		photoperiodic flowering, encodes an Arabidopsis GI ortholog. Plant Mol. Biol. 58, 53-64 (2005).
799	18.	Zikhali, M., Wingen, L. U. & Griffiths, S. Delimitation of the Earliness per se D1 (Eps-D1) flowering
800		gene to a subtelomeric chromosomal deletion in bread wheat (Triticum aestivum). J. Exp. Bot. 67, 287-
801		299 (2016).
802	19.	Wang, J. et al. TaELF3-1DL, a homolog of ELF3, is associated with heading date in bread wheat. Mol.
803		<i>Breed.</i> <b>36</b> , 1–9 (2016).
804	20.	Mizuno, N., Nitta, M., Sato, K. & Nasuda, S. A wheat homologue of PHYTOCLOCK 1 is a candidate
805		gene conferring the early heading phenotype to einkorn wheat. Genes Genet. Syst. 87, 357-367 (2012).
806	21.	Zhang, W. et al. Functional studies of heading date-related gene TaPRR73, a paralog of ppd1 in
807		common wheat. Front. Plant Sci. 7, 772 (2016).
808	22.	Dodd, A. N. et al. Plant circadian clocks increase photosynthesis, growth, survival, and competitive
809		advantage. Science (80 ). 309, 630-633 (2005).
810	23.	Graf, A., Schlereth, A., Stitt, M. & Smith, A. M. Circadian control of carbohydrate availability for
811		growth in Arabidopsis plants at night. Proc. Natl. Acad. Sci. U. S. A. 107, 9458-9463 (2010).
812	24.	Harmer, S. L. et al. Orchestrated transcription of key pathways in Arabidopsis by the circadian clock.
813		<i>Science (80 ).</i> <b>290</b> , 2110–3 (2000).
814	25.	Millar, A. J. & Kay, S. A. Circadian Control of cab Gene Transcription and mRNA Accumulation in
815		Arabidopsis. Plant Cell 3, 541-550 (1991).
816	26.	Romanowski, A., Schlaen, R. G., Perez-Santangelo, S., Mancini, E. & Yanovsky, M. J. Global
817		transcriptome analysis reveals circadian control of splicing events in Arabidopsis thaliana. Plant J. 103,
818		889–902 (2020).
819	27.	MacKinnon, K. J. M. et al. Changes in ambient temperature are the prevailing cue in determining
820		Brachypodium distachyon diurnal gene regulation. New Phytol. 227, 1709–1724 (2020).

821 28. Li, M. et al. Comprehensive mapping of abiotic stress inputs into the soybean circadian clock. Proc.

822		Natl. Acad. Sci. 116, 23840–23849 (2019).
823	29.	Greenham, K. et al. Expansion of the circadian transcriptome in Brassica rapa and genome-wide
824		diversification of paralog expression patterns. Elife 9, 1-68 (2020).
825	30.	Ramírez-González, R. H. et al. The transcriptional landscape of polyploid wheat. Science (80 ). 361,
826		(2018).
827	31.	Zhao, J. et al. Genome-Wide Identification and Expression Profiling of the TCP Family Genes in Spike
828		and Grain Development of Wheat (Triticum aestivum L.). Front. Plant Sci. 9, (2018).
829	32.	Takumi, S., Shimamura, C. & Kobayashi, F. Increased freezing tolerance through up-regulation of
830		downstream genes via the wheat CBF gene in transgenic tobacco. Plant Physiol. Biochem. 46, 205-211
831		(2008).
832	33.	Jouffe, C. et al. The Circadian Clock Coordinates Ribosome Biogenesis. PLoS Biol. 11, 1001455
833		(2013).
834	34.	Correa, A. et al. Multiple oscillators regulate circadian gene expression in Neurospora. Proc. Natl.
835		Acad. Sci. 100, 13597–13602 (2003).
836	35.	Mao, G., Seebeck, T., Schrenker, D. & Yu, O. CYP709B3, a cytochrome P450 monooxygenase gene
837		involved in salt tolerance in Arabidopsis thaliana. BMC Plant Biol. 13, 1-13 (2013).
838	36.	Pan, Y. et al. Cytochrome P450 monooxygenases as reporters for circadian-regulated pathways. Plant
839		Physiol. 150, 858–878 (2009).
840	37.	Spitzer, C. et al. The ESCRT-Related CHMP1A and B Proteins Mediate Multivesicular Body Sorting of
841		Auxin Carriers in Arabidopsis and Are Required for Plant Development. Plant Cell 21, 749-766 (2009).
842	38.	Bao, Y. et al. The tumor necrosis factor receptor-associated factor (TRAF)-like family protein SEVEN
843		IN ABSENTIA 2 (SINA2) promotes drought tolerance in an ABA-dependent manner in Arabidopsis.
844		New Phytol. 202, 174–187 (2014).
845	39.	Noordermeer, M. A., Veldink, G. A. & Vliegenthart, J. F. G. Fatty acid hydroperoxide lyase: A plant
846		cytochrome P450 enzyme involved in wound healing and pest resistance. ChemBioChem 2, 494–504
847		(2001).
848	40.	Murakami, M., Ashikari, M., Miura, K., Yamashino, T. & Mizuno, T. The Evolutionarily Conserved
849		OsPRR Quintet: Rice Pseudo-Response Regulators Implicated in Circadian Rhythm. Plant Cell Physiol.
850		<b>44</b> , 1229–1236 (2003).
851	41.	Shalit-Kaneh, A., Kumimoto, R. W., Filkov, V. & Harmer, S. L. Multiple feedback loops of the
852		Arabidopsis circadian clock provide rhythmic robustness across environmental conditions. Proc. Natl.
853		Acad. Sci. U. S. A. 115, 7147–7152 (2018).
854	42.	Hsu, P. Y., Devisetty, U. K. & Harmer, S. L. Accurate timekeeping is controlled by a cycling activator
855		in Arabidopsis. <i>Elife</i> <b>2013</b> , 473 (2013).
856	43.	Hou, X., Fu, A., Garcia, V. J., Buchanan, B. B. & Luan, S. PSB27: A thylakoid protein enabling
857		Arabidopsis to adapt to changing light intensity. Proc. Natl. Acad. Sci. 112, 1613-1618 (2015).
858	44.	Ponnu, J. & Hoecker, U. Illuminating the COP1/SPA Ubiquitin Ligase: Fresh Insights Into Its Structure
859		and Functions During Plant Photomorphogenesis. Front. Plant Sci. 0, 486 (2021).
860	45.	Jang, IC., Henriques, R. & Chua, NH. Three Transcription Factors, HFR1, LAF1 and HY5, Regulate
861		Largely Independent Signaling Pathways Downstream of Phytochrome A. Plant Cell Physiol. 54, 907-

862		916 (2013).
863	46.	Nakamura, Y., Kato, T., Yamashino, T., Murakami, M. & Mizuno, T. Characterization of a set of
864		phytochrome-interacting factor-like bHLH proteins in Oryza sativa. Biosci. Biotechnol. Biochem. 71,
865		1183–1191 (2007).
866	47.	Noordally, Z. B. et al. Circadian Control of Chloroplast Transcription by a Nuclear-Encoded Timing
867		Signal. Science (80 ). 339, 1316–1319 (2013).
868	48.	Tanaka, K. et al. Characterization of three cDNA species encoding plastid RNA polymerase sigma
869		factors in Arabidopsis thaliana: Evidence for the sigma factor heterogeneity in higher plant plastids.
870		FEBS Lett. 413, 309–313 (1997).
871	49.	Kanamaru, K. et al. Plastidic RNA polymerase o factors in Arabidopsis. Plant Cell Physiol. 40, 832-
872		842 (1999).
873	50.	Allison, L. A. The role of sigma factors in plastid transcription. Biochimie vol. 82 537-548 (2000).
874	51.	Kanamaru, K. & Tanaka, K. Roles of chloroplast RNA polymerase sigma factors in chloroplast
875		development and stress response in higher plants. Biosci. Biotechnol. Biochem. 68, 2215-2223 (2004).
876	52.	Shimizu, M. et al. Sigma factor phosphorylation in the photosynthetic control of photosystem
877		stoichiometry. Proc. Natl. Acad. Sci. U. S. A. 107, 10760-10764 (2010).
878	53.	Figueroa, C. M. & Lunn, J. E. A tale of two sugars: Trehalose 6-phosphate and sucrose. Plant
879		<i>Physiology</i> vol. 172 7–27 (2016).
880	54.	Frank, A. et al. Circadian Entrainment in Arabidopsis by the Sugar-Responsive Transcription Factor
881		bZIP63. Curr. Biol. 28, 2597-2606.e6 (2018).
882	55.	Fichtner, F. & Lunn, J. E. The Role of Trehalose 6-Phosphate (Tre6P) in Plant Metabolism and
883		Development. Annu. Rev. Plant Biol. 72, 737–760 (2021).
884	56.	Paul, M. J., Gonzalez-Uriarte, A., Griffiths, C. A. & Hassani-Pak, K. The Role of Trehalose 6-
885		Phosphate in Crop Yield and Resilience. Plant Physiol. 177, 12-23 (2018).
886	57.	Gruber, A. V. & Feiz, L. Rubisco assembly in the chloroplast. Frontiers in Molecular Biosciences vol. 5
887		24 (2018).
888	58.	Bhat, J. Y., Thieulin-Pardo, G., Hartl, F. U. & Hayer-Hartl, M. Rubisco activases: AAA+ chaperones
889		adapted to enzyme repair. Frontiers in Molecular Biosciences vol. 4 20 (2017).
890	59.	Smith, S. M. et al. Diurnal changes in the transcriptome encoding enzymes of starch metabolism
891		provide evidence for both transcriptional and posttranscriptional regulation of starch metabolism in
892		arabidopsis leaves. Plant Physiol. 136, 2687-2699 (2004).
893	60.	Periappuram, C. et al. The Plastidic Phosphoglucomutase from Arabidopsis. A Reversible Enzyme
894		Reaction with an Important Role in Metabolic Control. Plant Physiol. 122, 1193 (2000).
895	61.	Bahaji, A. et al. Plastidic phosphoglucose isomerase is an important determinant of starch accumulation
896		in mesophyll cells, growth, photosynthetic capacity, and biosynthesis of plastidic cytokinins in
897		Arabidopsis. PLoS One 10, e0119641 (2015).
898	62.	Lee, S. K. et al. Plastidic phosphoglucomutase and ADP-glucose pyrophosphorylase mutants impair
899		starch synthesis in rice pollen grains and cause male sterility. J. Exp. Bot. 67, 5557–5569 (2016).
900	63.	Nielsen, M. M. et al. Crystal structures of the catalytic domain of Arabidopsis thaliana starch synthase
901		IV, of granule bound starch synthase from CLg1 and of granule bound starch synthase I of Cyanophora

902		paradoxa illustrate substrate recognition in starch synthases. Front. Plant Sci. 9, 1138 (2018).
903	64.	Tenorio, G., Orea, A., Romero, J. M. & Mérida, Á. Oscillation of mRNA level and activity of granule-
904		bound starch synthase I in Arabidopsis leaves during the day/night cycle. Plant Mol. Biol. 51, 949-958
905		(2003).
906	65.	Yamamori, M., Nakamura, T., Endo, T. R. & Nagamine, T. Waxy protein deficiency and chromosomal
907		location of coding genes in common wheat. Theor. Appl. Genet. 89, 179-184 (1994).
908	66.	Vrinten, P. L. & Nakamura, T. Wheat granule-bound starch synthase I and II are encoded by separate
909		genes that are expressed in different tissues. Plant Physiol. 122, 255-263 (2000).
910	67.	Kaplan, F., Sung, D. Y. & Guy, C. L. Roles of β-amylase and starch breakdown during temperatures
911		stress. Physiol. Plant. 126, 120–128 (2006).
912	68.	Otto, S. P. The Evolutionary Consequences of Polyploidy. Cell 131, 452-462 (2007).
913	69.	Gardiner, L. J. et al. A genome-wide survey of DNA methylation in hexaploid wheat. Genome Biol. 16,
914		1–15 (2015).
915	70.	Chen, Z. J. & Mas, P. Interactive roles of chromatin regulation and circadian clock function in plants.
916		<i>Genome Biol.</i> <b>20</b> , 1–12 (2019).
917	71.	Walsh, J. B. How often do duplicated genes evolve new functions? Genetics 139, 421-428 (1995).
918	72.	Lou, P. et al. Preferential retention of circadian clock genes during diploidization following whole
919		genome triplication in Brassica rapa. Plant Cell 24, 2415-2426 (2012).
920	73.	Rees, H. et al. A high-throughput delayed fluorescence method reveals underlying differences in the
921		control of circadian rhythms in Triticum aestivum and Brassica napus. Plant Methods 15, 51 (2019).
922	74.	Yarkhunova, Y. et al. Selection during crop diversification involves correlated evolution of the
923		circadian clock and ecophysiological traits in Brassica rapa. New Phytol. 210, 133-144 (2016).
924	75.	Michael, T. P. et al. Enhanced Fitness Conferred by Naturally Occurring Variation in the Circadian
925		Clock. Science (80 ). 302, 1049–1053 (2003).
926	76.	Gould, P. D. et al. Coordination of robust single cell rhythms in the Arabidopsis circadian clock via
927		spatial waves of gene expression. Elife 7, (2018).
928	77.	Takahashi, N., Hirata, Y., Aihara, K. & Mas, P. A Hierarchical Multi-oscillator Network Orchestrates
929		the Arabidopsis Circadian System. Cell 163, 148-159 (2015).
930	78.	Locke, J. C. W. et al. Experimental validation of a predicted feedback loop in the multi-oscillator clock
931		of Arabidopsis thaliana. Mol. Syst. Biol. 2, 59 (2006).
932	79.	Hall, A., Kozma-Bognár, L., Bastow, R. M., Nagy, F. & Millar, A. J. Distinct regulation of CAB and
933		PHYB gene expression by similar circadian clocks. Plant J. 32, 529-537 (2002).
934	80.	Hotta, C. T. et al. Are there multiple circadian clocks in plants? Plant Signal. Behav. 3, 342 (2008).
935	81.	Cuitun-Coronado, D., Rees, H., Hall, A., de Barros Dantas, L. L. & Dodd, A. N. Circadian and diel
936		regulation of photosynthesis in the bryophyte Marchantia polymorpha. bioRxiv (2022)
937		doi:10.1101/2022.01.11.475783.
938	82.	Cano-Ramirez, D., Fraine, T., Griffiths, O. & Dodd, A. Photosynthesis and circadian rhythms regulate
939		the buoyancy of marimo lake balls. Curr. Biol. 28, R869-R870 (2018).
940	83.	Schneegurt, M. A., Tucker, D. L., Ondr, J. K., Sherman, D. M. & Sherman, L. A. Metabolic rhythms of
941		a diazotrophic cyanobacterium, cyanothece sp. strain atcc 51142, heterotrophically grown in continuous

942		dark. J. Phycol. 36, 107–117 (2000).
943	84.	Delorge, I., Figueroa, C. M., Feil, R., Lunn, J. E. & Van Dijck, P. Trehalose-6-phosphate synthase 1 is
944		not the only active TPS in Arabidopsis thaliana. Biochem. J. 466, 283-290 (2015).
945	85.	Tian, L. et al. The trehalose-6-phosphate synthase TPS5 negatively regulates ABA signaling in
946		Arabidopsis thaliana. Plant Cell Rep. 38, 869-882 (2019).
947	86.	Suzuki, N., Bajad, S., Shuman, J., Shulaev, V. & Mittler, R. The Transcriptional Co-activator MBF1c Is
948		a Key Regulator of Thermotolerance in Arabidopsis thaliana. J. Biol. Chem. 283, 9269-9275 (2008).
949	87.	Wang, X., Du, Y. & Yu, D. Trehalose phosphate synthase 5-dependent trehalose metabolism modulates
950		basal defense responses in Arabidopsis thaliana. J. Integr. Plant Biol. 61, 509-527 (2019).
951	88.	V, S. et al. TREHALOSE PHOSPHATE SYNTHASE11-dependent trehalose metabolism promotes
952		Arabidopsis thaliana defense against the phloem-feeding insect Myzus persicae. Plant J. 67, 94-104
953		(2011).
954	89.	Vishal, B., Krishnamurthy, P., Ramamoorthy, R. & Kumar, P. P. OsTPS8 controls yield-related traits
955		and confers salt stress tolerance in rice by enhancing suberin deposition. New Phytol. 221, 1369-1386
956		(2019).
957	90.	Liu, X. et al. Overexpression of the wheat trehalose 6-phosphate synthase 11 gene enhances cold
958		tolerance in Arabidopsis thaliana. Gene 710, 210-217 (2019).
959	91.	Bolger, A. M., Lohse, M. & Usadel, B. Trimmomatic: A flexible trimmer for Illumina sequence data.
960		<i>Bioinformatics</i> <b>30</b> , (2014).
961	92.	Kim, D., Paggi, J. M., Park, C., Bennett, C. & Salzberg, S. L. Graph-based genome alignment and
962		genotyping with HISAT2 and HISAT-genotype. Nat. Biotechnol. 37, (2019).
963	93.	Pertea, M., Kim, D., Pertea, G. M., Leek, J. T. & Salzberg, S. L. Transcript-level expression analysis of
964		RNA-seq experiments with HISAT, StringTie and Ballgown. Nat. Protoc. 11, (2016).
965	94.	Gardiner, L. J. et al. Interpreting machine learning models to investigate circadian regulation and
966		facilitate exploration of clock function. Proc. Natl. Acad. Sci. U. S. A. 118, 2021 (2021).
967	95.	Zhang, H. et al. A Comprehensive Online Database for Exploring ∼20,000 Public
968		<em>Arabidopsis</em> RNA-Seq Libraries. Mol. Plant 13, 1231–1233 (2020).
969	96.	Eddy, S. R. Accelerated Profile HMM Searches. PLOS Comput. Biol. 7, e1002195 (2011).
970	97.	Stamatakis, A. RAxML version 8: a tool for phylogenetic analysis and post-analysis of large
971		phylogenies. Bioinformatics 30, 1312-1313 (2014).
972	98.	Letunic, I. & Bork, P. Interactive tree of life (iTOL) v3: an online tool for the display and annotation of
973		phylogenetic and other trees. Nucleic Acids Res. 44, W242-W245 (2016).
974	99.	Smedley, D. et al. BioMart – biological queries made easy. BMC Genomics 2009 101 10, 1–12 (2009).
975	100.	Kim, J. A. et al. Transcriptome analysis of diurnal gene expression in Chinese cabbage. Genes (Basel).
976		<b>10</b> , (2019).
977	101.	Yang, Y., Li, Y., Sancar, A. & Oztas, O. The circadian clock shapes the Arabidopsis transcriptome by
978		regulating alternative splicing and alternative polyadenylation. J. Biol. Chem. 295, 7608–7619 (2020).
979	102.	Wu, G., Anafi, R. C., Hughes, M. E., Kornacker, K. & Hogenesch, J. B. MetaCycle: an integrated R
980		package to evaluate periodicity in large scale data. Bioinformatics 32, 3351-3353 (2016).
981	103.	Agostinelli, C. & Lund, U. R package 'circular': Circular Statistics. (2017).

982	104.	Zielinski, T., Moore, A. M., Troup, E., Halliday, K. J. & Millar, A. J. Strengths and Limitations of
983		Period Estimation Methods for Circadian Data. PLoS One 9, e96462 (2014).
984	105.	Alexa, A. & Rahnenfuhrer, J. topGO: Enrichment Analysis for Gene Ontology. R package version
985		2.44.0. <i>Alexa</i> (2021).
986	106.	De Vega, J. J. et al. Differential expression of starch and sucrose metabolic genes linked to varying
987		biomass yield in Miscanthus hybrids. Biotechnol. Biofuels 14, 98 (2021).
988	107.	O'Malley, R. C. et al. Cistrome and Epicistrome Features Shape the Regulatory DNA Landscape. Cell
989		<b>165</b> , (2016).
990	108.	Marcussen, T. et al. Ancient hybridizations among the ancestral genomes of bread wheat. Science (80
991		). <b>345</b> , 6194 (2014).
992	109.	Zeeman, S. C., Smith, S. M. & Smith, A. M. The diurnal metabolism of leaf starch. Biochem. J. 401,
993		13–28 (2007).
994	110.	López-González, C., Juárez-Colunga, S., Morales-Elías, N. C. & Tiessen, A. Exploring regulatory
995		networks in plants: Transcription factors of starch metabolism. PeerJ 2019, e6841 (2019).
996	111.	Skryhan, K., Gurrieri, L., Sparla, F., Trost, P. & Blennow, A. Redox regulation of starch metabolism.
997		Front. Plant Sci. 9, 1344 (2018).
998		
999		
1000		
1001		
1001		

#### 1002 Acknowledgements

- 1003 H.R., R.R.P. and A.H. were funded by the BBSRC Core Strategic Programme Grant
- 1004 (Genomes to Food Security) BB/CSP1720/1 and its constituent work package,
- 1005 BBS/E/T/000PR9819 (WP2 Regulatory interactions and Complex Phenotypes). B.W., R.R.P.
- and A.H. was supported by the BBSRC Designing Future Wheat grant BB/P016855/1;
- 1007 BBS/E/T/000PR9783 (DFW WP4 Data Access and Analysis). C.R. by a BBSRC grant
- 1008 BB/V509267/1 and Wave 1 of The UKRI Strategic Priorities Fund under the EPSRC Grant
- 1009 EP/T001569/1, particularly the "AI for Science" theme within that grant & The Alan Turing
- 1010 Institute. J.C. by the BBSRC funded Norwich Research Park Biosciences Doctoral Training
- 1011 Partnership grant BB/M011216/1. We would also like to acknowledge BBS/E/T/000PR9816
- 1012 (NC1 Supporting EI's ISPs and the UK Community with Genomics and Single Cell
- 1013 Analysis) for data generation and BB/CCG1720/1 for the physical HPC infrastructure and
- 1014 data centre delivered via the NBI Computing infrastructure for Science (CiS) group. P.B. was
- 1015 supported by a BBSRC TRDF grant BB/N023145/1. A.N.D., L.L.B.D. and C.A.G. are
- 1016 funded by BBSRC ISP Genes in the Environment (BB/P013511/1). C.A.G. was also funded
- 1017 by UK BBSRC SWBIO DTP (BB/M009122/1). We thank Dr. Susan Duncan for her
- 1018 contribution to preliminary experiments prior to the start of this project.
- 1019
- 1020

# 1021 Author contributions

- H.R. and A.H. were involved with project concept and designed experiments. H.R. performed
  time-course experiments. R.R.P. processed data, quantified read counts and conducted
- 1023 unit course experiments. Rikir : processed dudi, quantified feud courts and conducted
- 1024 clustering of rhythmic transcripts. P.B. conducted the phylogenetic analysis of core circadian
- 1025 protein families. J.C. conducted the cross-correlation analysis. C.R. processed previously
- 1026 published circadian datasets. S.J.W produced loom plots for circadian triad balance. H.R.,
- 1027 L.L.B.D., C.A.G., B.W., R.R.P. A.H., and A.N.D. analysed and interpreted the RNA-seq
- 1028 data. H.R. wrote the initial manuscript and all authors contributed to subsequent drafts.
- 1029
- 1030 Corresponding author
- 1031 Correspondence to Anthony Hall.
- 1032
- 1033 Ethics declarations
- 1034 Competing interests: The authors declare no competing interests.

# 1035 Main Figures and Tables

# 1036 [Figures are provided as separate files]

#### 1037 Fig. 1. Circadian regulation of homoeolog expression of wheat triads.

1038 a, Schematic of the origins of hexaploid wheat, showing circadian clocks evolving 1039 independently in the ancestors of the A, B and D subgenomes following divergence from a 1040 common ancestor approximately 6.5 million years ago. Colours of clock icons represent 1041 theoretical differences in clock regulation integrated in the tetraploid and hexaploid hybrids either through circadian balance or through dominance of a particular homoeolog copy. 1042 Speciation and hybridisation event dates are based on estimates from<sup>108</sup>. **b**, Density plot 1043 showing the distribution of period lengths across rhythmic transcripts (BH q < 0.01) in 1044 1045 Arabidopsis, Brassica rapa, Brachypodium distachyon, Glycine max (Soybean) and wheat based on meta2d estimates on 24-68h data following transfer to constant light. c, Histogram 1046 1047 showing distribution of period lengths in wheat split between the A, B and D subgenomes. 1048 Dotted line indicates the mean period for the A, B and D subgenomes. d, Proportions of triads 1049 with either zero (red segment), one (green segment), two (blue segment) or three (purple segment) rhythmic gene(s) out of the 16,359 expressed triads in this dataset. Lighter shading 1050 1051 in the outer segments represents cases where one/two homeolog(s) have high confidence 1052 rhythmicity (BH q < 0.01) alongside an arrhythmic homeolog (BH q > 0.05). We term these 1053 genes "imbalanced rhythmicity" triads. Of the 3448 triads with three rhythmic genes 1054 (represented by the purple segment in d), we also looked for triads with circadian imbalance in: phase (e), period (f) or relative amplitude (g). 464 triads had homoeologs which peaked 1055 1056 with an optimum lag of 4, 8 or 12h following cross-correlation analysis. 1,139 triads had homoeologs with period differences of more than 2h. 701 triads had homoeologs with a more 1057 than two-fold difference in relative amplitude. **h**,**i**, Example triads for imbalanced rhythmicity, 1058 1059 where either one or two homoeologs are rhythmic respectively. **j**, Example triad where the D genome homeolog lags by 8h. k, Example of a triad where the A genome homoeolog has a 1060 period estimate 4h longer than the D genome homoeolog. I, Example triad where the relative 1061 1062 amplitude of the D-genome homoeolog is more than four times that of the A-genome homoeolog. **m**, The rhythmicity of all three homoeologs in **l**, is evident when the expression is 1063 1064 mean normalized. n, Mean expression of transcripts across all timepoints in the A, B and D 1065 subgenomes within imbalanced rhythmicity triads compared with circadian balanced and 1066 arrhythmic triads. Error bars represent standard error.

1067 Circadian statistics are meta2d estimates from data 0-68h after transfer to L:L. Data represent the mean of three biological replicates with transcript expression collapsed to gene level. Genes 1068 in example triads are: [Triad 1664: TraesCS3A02G177600, TraesCS3B02G207400, 1069 1070 TraesCS3D02G183200], [Triad 408: TraesCS3A02G533700, TraesCS3B02G610500, 1071 TraesCS3D02G539000], [Triad 13405: TraesCS6A02G269100, TraesCS6B02G296400, TraesCS6D02G245800], [Triad 10854: TraesCS6A02G166500, TraesCS6B02G194000, 1072 1073 TraesCS6D02G155100] and [Triad 2454: TraesCS2A02G333000, TraesCS2B02G348800, 1074 TraesCS2D02G329900].

- 1076
- 1077

# 1078 Fig. 2. Overlapping GO-slim terms shared between *Arabidopsis* and wheat modules

# 1079 expressed at similar times in the day

1080 a, Pearson correlation coefficient (r) between eigengenes for wheat and Arabidopsis expression 1081 modules ordered by circadian phase. Coloured triangles and axes labels correspond to module expression profiles and columns in bubble-plot. b-e, Expression profiles of Arabidopsis and 1082 wheat modules compared in the main text normalised to their mean. Solid and dashed black 1083 1084 lines represent the module eigengene for wheat and Arabidopsis modules respectively. f, GOslim terms associated with Arabidopsis and Wheat modules. Modules are ordered by predicted 1085 CT phase for each species. Only terms with -Log10p > 3 are shown. Wheat W6 and *Arabidopsis* 1086 A4 contained no terms above the significance cut-off and so are not shown. Bubble color 1087 indicates the -Log10p-value significance from Fisher's exact test and size indicates the 1088 1089 frequency of the GO-slim term in the underlying EBI Gene Ontology Annotation database 1090 (larger bubbles indicate more general terms). 1091

## 1093 Fig. 3. Free-running expression of core circadian clock genes in wheat and their homologs

1094 in Arabidopsis. a-l, Wheat circadian clock genes were identified through alignment of

1095 phylogenetic protein family trees or BLASTP to known clock gene homologs. Gene IDs for

each gene set are in Supplementary Table 8. Wheat homoeologs are coloured according to theiridentity to either the A genome (orange), B genome (yellow) or D genome (blue) and grey and

1097 Identity to efficience (orange), B genome (orange), B genome (orange) and grey and 1098 white blocks indicate subjective dark and light time periods under constant conditions. Data

1099 represent the mean of three biological replicates and transcript expression is collapsed to gene

- 1100 level. Expression profiles for additional core circadian clock genes are in Supplementary Fig.
- 1101 17. **m**, phases of core clock genes in *Arabidopsis* and wheat (meta2d estimates from data 24-
- 1102 68h after transfer to L:L). Genes were not plotted if B.H q-values were > 0.01. Wheat values

1103 represent circular mean circadian phases (CT) across homoeologs calculated in Supplementary1104 Table 9.

# 1106 Fig. 4. Similarities and differences in circadian control of transcript accumulation in key

1107 genes involved in primary metabolism and signalling. Circles represent metabolites 1108 involved in the breakdown and biosynthesis of starch. Starch synthesis occurs during the day 1109 and breakdown occurs at night as indicated by the yellow to grey shading gradient. The dotted 1110 line encloses processes which take place in the chloroplast. Abbreviations: HP: Hexose-1111 phosphate, T6P: Trehalose-6-phosphate, TP: Triose phosphate, 3-PGA: Glycerate 3-1112 phosphate, Fru6P: Fructose-6-phosphate, Glc6P: Glucose-6-phosphate, Glc1P: Glucose-1-1113 phosphate, ATP: Adensoine tri phosphate, ADP-Glc: ADP-glucose, TPS: Trehalose phosphate 1114 synthase, TPP: Trehalose phosphate phosphatase, PGK1: Phosphoglycerate kinase 1, PGI1: 1115 Glucose-6-phosphate isomerase, PGM1: Phosphoglucomutase-1, PHS1 and 2: ALPHA-GLUCAN PHOSPHORYLASE 1 and 2, AGPase: ADP-Glc pyrophosphorylase, BAM1,3,5: 1116 1117 β-amylase 1,3,5, ISA1,2,3: Isoamylase 1,2,3, DPE1,2: Disproportionating enzyme1 and 2, 1118 SBEI,II: Starch branching enzyme I, II, PU1: Pullulanase 1, PWD: Phosphoglucan, water 1119 dikinase, GWD: α-glucan, water dikinase, SEX4: starch excess 4, AMY3: α-amylase, GBSS: Granule bound Starch synthase, SSI-IV: Starch synthase I-IV. Pathway references:<sup>109–111</sup>. 1120

# 1122 Table 1: Numbers of rhythmic genes at (BH q < 0.05 or BH q < 0.01) in *Arabidopsis* and

1123 wheat identified using Metacycle Benjamini Hochberg q-values. Periods, relative

amplitudes, and q-values are estimates from meta2d. Data windows reflect hours relative to

- 1125 transfer to constant light from entrained 12:12h light conditions. A repeat of this table with
- 1126 pre-filtering to remove low-expression genes is provided in Supplementary Figure 1, and the
- effects on proportions of rhythmic genes are discussed in Supplementary Note 1.
- 1128

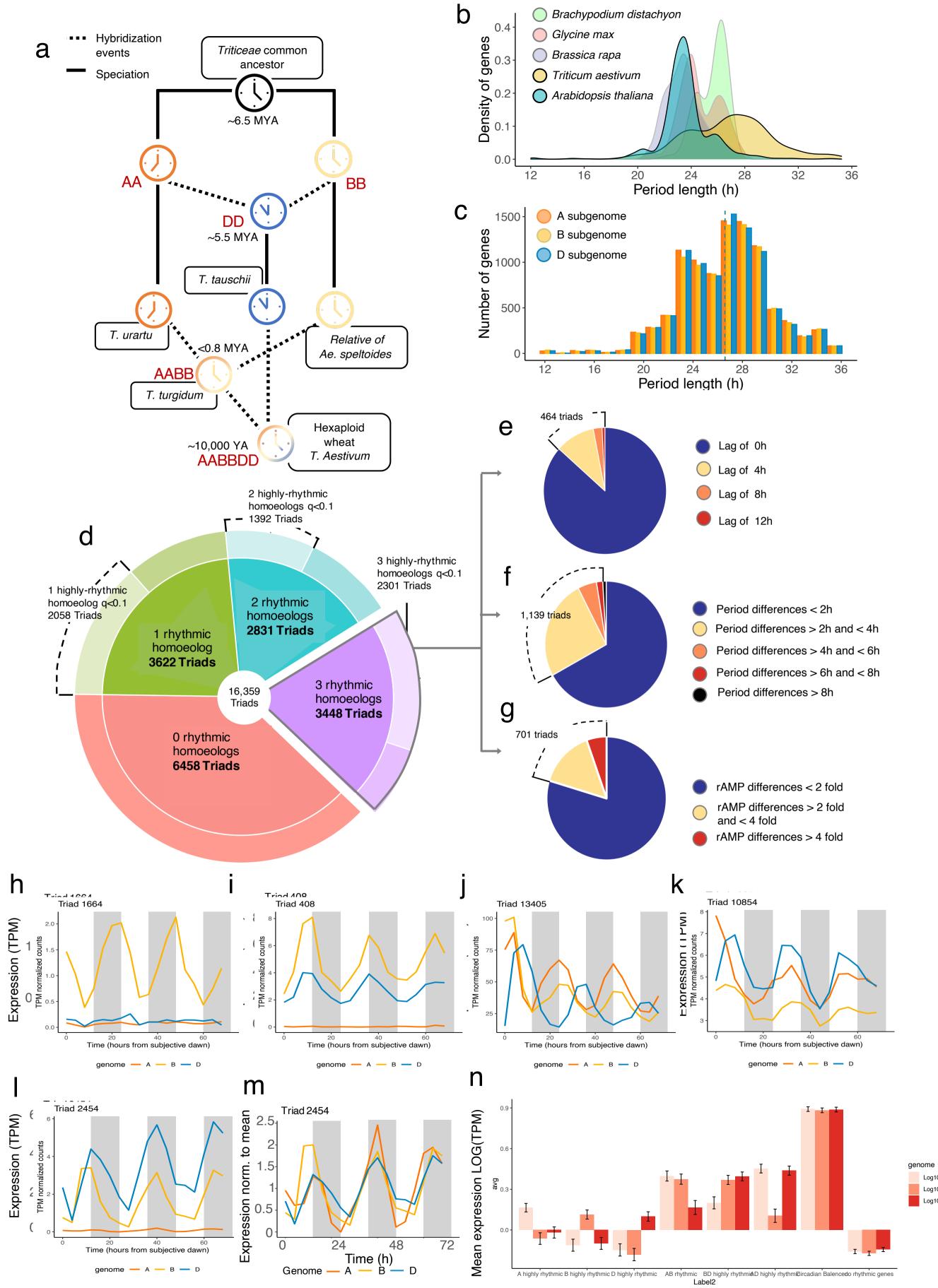
	Wheat data from	n this study	<i>Arabidopsis</i> data from Romanowski et al.		
	24-68 data window	0-68 data window	24-68 data window		
Total number of expressed genes	86,567	86,567	26,392		
Total rhythmic genes (BH $q < 0.05$ )	28,594	28,530	13,392		
Total rhythmic genes (BH $q < 0.01$ )	18,633	21,059	10,317		
Mean Period (h) (BH q < 0.05)	26.60h (SD 3.62)	26.75h (SD 2.82)	23.50 (SD 2.52)		
Mean Period (h) (BH q < 0.01)	26.82h (SD 3.21)	26.83h (SD 2.42)	23.62 (SD 2.04)		
Mean relative Amplitude (BH $q < 0.05$ )	0.24 (SD 0.19)	0.26 (SD 0.20)	0.28 (SD 0.20)		
Mean relative Amplitude (BH $q < 0.01$ )	0.27 (SD 0.19)	0.29 (SD 0.21)	0.30 (SD 0.20)		

# 1129 Table 2: GO-slim terms for biological processes associated with circadian balanced,

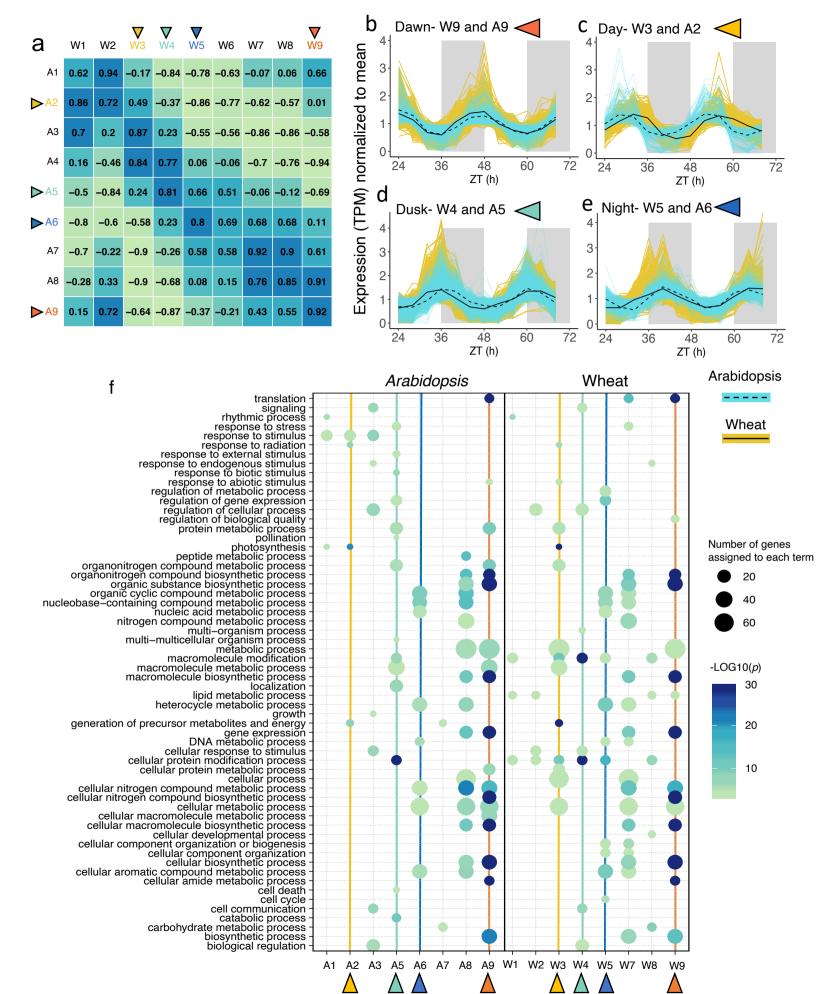
- 1130 circadian imbalanced, and arrhythmic wheat triads. Only enriched terms which were
- 1131 highly enriched (Fisher's exact test p < 0.01) in one category and non-significantly expressed
- 1132 (p>0.05) in other categories is displayed.

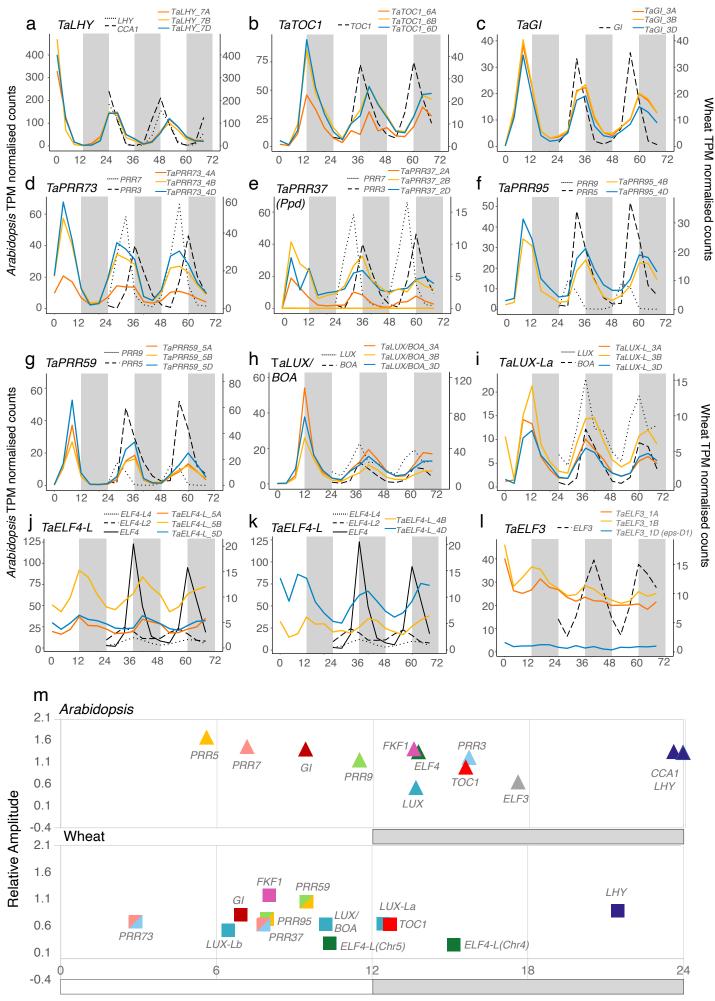
			<i>p</i> -value		
			in		
			circadia	<i>p</i> -value in	<i>p</i> -value
			n	circadian	in non-
			balance	imbalance	rhythmi
	GO ID	Terms	d triads	d triads	c triads
	GO:0009628	response to abiotic stimulus	0.00	0.22	0.58
	GO:0015979	photosynthesis	0.00	1.00	1.00
		generation of precursor metabolites and			
	GO:0006091	energy	0.00	1.00	1.00
	GO:0006518	peptide metabolic process	0.00	1.00	0.92
		organonitrogen compound biosynthetic			
CIRCADIAN	GO:1901566	process	0.00	1.00	0.92
BALANCED	GO:0009059	macromolecule biosynthetic process	0.00	1.00	0.99
	GO:0006412	translation	0.00	1.00	0.98
		cellular macromolecule biosynthetic			
	GO:0034645	process	0.00	1.00	1.00
	GO:0010467	gene expression	0.00	1.00	0.90
	GO:0019725	cellular homeostasis	0.00	0.54	0.96
	GO:0065008	regulation of biological quality	0.00	0.71	1.00
		developmental process involved in			
	GO:0003006	reproduction	0.85	0.00	0.87
	GO:0090567	reproductive shoot system development	0.92	0.01	1.00
CIRCADIAN IMBALANCE	GO:0009719	response to endogenous stimulus	0.97	0.01	0.10
D	GO:0048731	system development	0.98	0.00	0.97
D	GO:0048608	reproductive structure development	0.98	0.00	0.97
	GO:0043412	macromolecule modification	1.00	0.00	0.28
	GO:0022414	reproductive process	1.00	0.00	0.47
	GO:0044237	cellular metabolic process	0.08	1.00	0.00
	GO:0009605	response to external stimulus	0.41	0.39	0.00
NON-	GO:0009607	response to biotic stimulus	0.58	0.60	0.01
RHYTHMIC		regulation of macromolecule metabolic			
	GO:0060255	process	0.60	0.76	0.00
	GO:0009056	catabolic process	0.65	0.93	0.00

GO:0048869	cellular developmental process	0.71	0.19	0.00
GO:0019222	regulation of metabolic process	0.78	0.85	0.00
GO:0044238	primary metabolic process	0.81	0.24	0.00
GO:0071704	organic substance metabolic process	0.81	0.26	0.00
GO:0008219	cell death	0.82	0.94	0.00
GO:0010468	regulation of gene expression	0.88	0.15	0.00
GO:0009790	embryo development	0.95	0.98	0.00
GO:0007049	cell cycle	0.97	1.00	0.00
GO:0065009	regulation of molecular function	1.00	1.00	0.00
GO:0006807	nitrogen compound metabolic process	1.00	1.00	0.00



Laiaiiooa





Circadian phase (h from dawn)

